

This is a repository copy of *Balancing cost-efficiency and sustainability in offshore hybrid renewable energy systems: A case study of Palau River*.

White Rose Research Online URL for this paper:

<https://eprints.whiterose.ac.uk/230117/>

Version: Published Version

Article:

Terkas, Musa, Syarif, Muhammad Rizqi Asy, Demirci, Alpaslan et al. (3 more authors) (2025) Balancing cost-efficiency and sustainability in offshore hybrid renewable energy systems: A case study of Palau River. *Energy Reports*. pp. 1095-1113. ISSN 2352-4847

<https://doi.org/10.1016/j.egyr.2025.06.053>

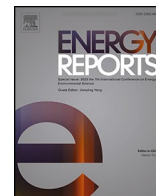
Reuse

This article is distributed under the terms of the Creative Commons Attribution (CC BY) licence. This licence allows you to distribute, remix, tweak, and build upon the work, even commercially, as long as you credit the authors for the original work. More information and the full terms of the licence here:

<https://creativecommons.org/licenses/>

Takedown

If you consider content in White Rose Research Online to be in breach of UK law, please notify us by emailing eprints@whiterose.ac.uk including the URL of the record and the reason for the withdrawal request.



Research paper

Balancing cost-efficiency and sustainability in offshore hybrid renewable energy systems: A case study of Palau River

Musa Terkes^a, Muhammad Rızqi Asy Syarif^a, Alpaslan Demirci^a, Zafer Ozturk^b,
Erdin Gokalp^a, Umit Cali^{c,d,*}

^a Department of Electrical Engineering, Yildiz Technical University, İstanbul, Türkiye

^b Department of Electrical and Electronic Engineering, Duzce University, Duzce, Türkiye

^c Department of Electric Energy, Norwegian University of Science and Technology, Trondheim, Norway

^d School of Physics, Engineering and Technology, University of York, York, United Kingdom

ARTICLE INFO

Keywords:

Carbon neutrality

Carbon tax

Floating solar

Offshore wind turbine

Optimization

Tidal/wave energy

ABSTRACT

Increasing environmental concerns and regulations on carbon emissions necessitate the development of economically viable and sustainable renewable energy systems. In this context, comprehensively evaluating solar PV-based hybrid energy systems under carbon tax (CT) scenarios is critically important. This study comparatively analyzes the cost-effectiveness, sustainability, and economic impacts of carbon taxation on both grid-connected and off-grid system configurations. Specifically, the effects of a CT on the costs of grid-connected system architectures are examined in detail, and cost reduction rates at various CTs are presented. By comparing different configurations in terms of technical performance and environmental benefits, optimal sizing strategies are determined to balance cost and carbon emissions. The results indicate that CT implementation provides a cost advantage in grid-connected systems, leading to a reduction in total system costs by approximately 15–22 %. Moreover, hybrid systems demonstrate significant improvements in environmental sustainability. These findings clearly highlight a critical role of CT policies in renewable energy integration and the economic and environmental benefits of hybrid energy systems.

1. Introduction

1.1. Motivation and Incentives

The increase in global energy demand is exacerbating the environmental impacts of fossil fuels and necessitating the transition to sustainable energy systems (Kazemi-Robati et al., 2024; Martinez and Iglesias, 2022). The integration of renewable energy systems presents a critical solution for ensuring environmental sustainability and reducing carbon emissions (Lilas et al., 2022). Hybrid systems enabled by the integration of renewable energy sources in offshore systems plays a crucial role in securing a sustainable energy future in the global energy transition. Offshore renewable energy, particularly the combined use of diversified sources such as wind, solar, and ocean energy, offers the potential to enhance energy production. These hybrid systems aim to optimize energy efficiency (Huang and Iglesias, 2024; Zhou et al., 2022) while reducing environmental impacts (Ghigo et al., 2020). The main advantage of offshore renewable energy systems is their ability to be

installed on the sea surface, making them particularly significant in regions with limited land use. Technologies such as offshore wind turbines (OWTs), floating solar photovoltaic (FSPV) systems, and wave energy converters (WECs) have the potential to enhance the efficiency of offshore energy production. For instance, floating wind turbines allow installations in deep seas, enabling a higher energy production capacity (Kowsar et al., 2023). The integration of these systems reduces the variability in energy production by utilizing the dynamics of the marine environment more efficiently (Alcañiz et al., 2024). However, while an integrated mechanism presents various environmental and operational challenges, the combined use of these resources significantly increases efficiency. In the long term, this also leads to lower energy production costs and enhanced competitiveness (Izquierdo-Pérez et al., 2020). For instance, the combined use of wind and solar energy balances the intermittent nature of energy, ensuring a more stable energy flow (Bi and Law, 2023; Kangaji et al., 2024). Similarly, the combination of wave energy and wind energy optimizes energy production by highlighting the strengths of both sources, while helping to reduce energy costs (Balta

* Corresponding author at: Department of Electric Energy, Norwegian University of Science and Technology, Trondheim, Norway.

E-mail address: umit.cali@ntnu.no (U. Cali).

<https://doi.org/10.1016/j.egy.2025.06.053>

Received 29 March 2025; Received in revised form 2 June 2025; Accepted 29 June 2025

Available online 21 July 2025

2352-4847/© 2025 The Authors. Published by Elsevier Ltd. This is an open access article under the CC BY license (<http://creativecommons.org/licenses/by/4.0/>).

and Yumurtaci, 2024; Ferrari et al., 2020; Görmüş et al., 2024). Offshore wind energy offers large capacity due to its high wind potential and, when combined with wave energy, provides more sustainable solutions (Petracca et al., 2022). The integrated mechanism working in the offshore environment is also considered a key strategy for enhancing energy security. The combination of wind and solar energy increases the continuity of energy production and balances the shortages of both sources (López et al., 2020). Additionally, the integration of energy storage systems (ESS) enhances the efficiency of these hybrid systems, providing more sustainable solutions (Varotto et al., 2024).

On the other hand, offshore hybrid energy systems, particularly those utilizing marine natural resources more efficiently, offer significant potential. These systems not only ensure local energy production but also provide broader energy supply security in grid-connected regions (Alex et al., 2022; Ramos-Marín et al., 2024). Such systems have significant potential to meet energy needs in remote areas far from major demand centers. However, the integration of offshore renewable energy systems also faces challenges. The main challenges include environmental factors such as sea conditions and saltwater resistance. Furthermore, the installation of such systems is typically associated with high costs and complex construction processes (Benjamins et al., 2024; Wen and Lin, 2024). Nevertheless, these challenges can be overcome through innovative engineering solutions and technological advancements. For instance, OWTs and FSPV show significant progress in providing higher energy production in deep seas (Golroodbari et al., 2021). However, further development of these technologies, along with continued research, is essential to reduce costs and mitigate environmental impacts (Cho et al., 2024). Ultimately, the diversification of renewable energy systems is a critical step in ensuring continuity in energy production and reducing environmental impacts (Li et al., 2022a). In this regard, the integration of offshore renewable energy projects is of great importance for contributing to the global energy transition and supporting environmental sustainability (Ghigo et al., 2022). This transition will play a key role in meeting future energy demands by providing sustainable solutions instead of fossil fuels (Bahadori et al., 2019).

1.2. Literature Review

In order to overcome the fundamental challenges of renewable energy systems, such as land constraints and production intermittency, offshore installations, especially in the form of hybrid systems, are gaining increasing prominence. In the literature, attention has been paid to capacity constraints of existing infrastructures (Kazemi-Robati et al., 2024), uncertainties in the integration of offshore resources and their fluctuating production profiles (Huang and Iglesias, 2024), and the optimal restructuring of these systems. The cost-effective sizing of floating platforms without compromising structural requirements (Ghigo et al., 2020) is particularly critical to enhance energy production efficiency under marine conditions. In this context, studies that examine the technical and economic feasibility of hybrid installations (e.g., FSPV + OWT + WEC), not only in open seas but also in challenging environments such as marshlands (Kowsar et al., 2023), highlight the need for careful analysis regarding site selection and infrastructure requirements. Design parameters such as tilt angle, which affect the stability of the installation, also significantly influence production continuity (Bi and Law, 2023). Furthermore, for effective operation of clean energy systems, the integration of energy storage becomes essential due to the intermittent nature of renewable resources. In this regard, incorporating energy storage systems into offshore platforms, particularly mobile ones, offers advantages in mitigating power fluctuations and ensuring supply security (Kangaji et al., 2024; Ramos-Marín et al., 2024). The optimization of hybrid storage models both onshore and offshore (Varotto et al., 2024) is strategically important in this context.

Moreover, the complementary nature of solar, wind, and wave

energy resources in various coastal regions (Balta and Yumurtaci, 2024; Satymov et al., 2024) necessitates region-specific resource integration strategies in system design. Indicators such as capacity factor, orientation, and power correlations (Görmüş et al., 2024) are crucial data sources for decision-makers in terms of hybrid system efficiency. Accordingly, hybrid configurations can offer hydrodynamic stability and lower energy generation costs compared to single technologies (Petracca et al., 2022). Integration of FSPV and OWT in deep waters increases energy density per unit sea surface (López et al., 2020), and economic assessments focused on levelized cost of energy (LCOE) for floating installations (Martinez and Iglesias, 2024a) reinforce their feasibility. The initial commercial applications of WECs, when integrated with wind energy through shared infrastructures, can also provide balancing effects in energy production (Rönkkö et al., 2023). In this context, evaluating not only offshore but also land-based installations from an integrated perspective (İpekli et al., 2024) can offer holistic solutions for urban-centered energy planning. However, the economic evaluation of offshore investments must be based on multi-parametric variables such as LCOE calculations, project lifetime, discount rate, and turbine costs (Martinez and Iglesias, 2021). Creating regional energy cost maps (Martinez and Iglesias, 2024b) provides strategic data for investment decisions, while factors such as distance from the shore, latitude, and water depth directly influence system design. For investment decisions in such energy conversion systems, the integration of microgrid architecture (Toms et al., 2023) and second-life batteries (SLB) (Zaman and Ongsakul, 2022) can make offshore installations more sustainable and suitable for integration into smart city transformation. On the other hand, using hybrid platforms based on the complementarity of renewable energy sources (e.g., wind + solar for production increase, wave + solar for continuity) (Vázquez et al., 2024) can ensure production stability and reduce storage needs. Therefore, the design of offshore hybrid energy systems requires a multi-dimensional planning approach regarding resource selection, storage integration, and control strategies. Studies in the literature, especially those focusing on spatial layout and design optimization (Jiang et al., 2023), emphasize detailed analyses of hybrid energy systems' geometric and orientation parameters. Parametric optimization processes (Neshat et al., 2024) should address both external (geometry) and internal (power extraction) levels to maximize energy production. Control strategies developed to meet power quality requirements such as frequency stability and voltage profile (Rasool et al., 2023, 2022) also enhance grid integration of these systems.

Although there has been an increase in studies on offshore installations, the commercial-scale deployment of these systems in the energy market remains limited. The primary reasons include high initial investment costs, maintenance and operational difficulties, the need to comply with environmental regulations, and infrastructure deficiencies. Additionally, technical uncertainties encountered in the integration of offshore hybrid systems and limitations in energy transmission also restrict the market effectiveness of these technologies. Despite the technical, economic, and environmental gains obtained through optimization, these challenges can limit the applicability of offshore systems, particularly in developing countries. However, with the integration of environmental cost mechanisms such as carbon tax (CT), the disadvantages of conventional energy production methods become more visible, and the relative advantages of renewable energy investments increase. This positions offshore hybrid systems as a more competitive option and lays the groundwork for their inclusion in long-term sustainable energy policies. As policies aimed at reducing carbon emissions gain importance, CT implementations have emerged as key tools accelerating energy transformation. While CTs increase the cost of conventional energy production methods, they make renewable energy investments more attractive and facilitate the energy transition (Colasante et al., 2022). In this regard, the role of CT in transforming the energy sector is significant (Gugler et al., 2023). However, it is frequently emphasized that CT alone is insufficient and must be supported by other incentive-based policies (Dong et al., 2022; Kafeel et al.,

2024; Smith, 2020). For instance, the carbon price support (CPS) tax implemented in the United Kingdom has encouraged a shift from coal to cleaner natural gas power plants, resulting in a 6.2 % reduction in carbon emissions (Abrell et al., 2022). Additionally, once CT reaches a certain level, it can significantly affect system performance (Ahmadi et al., 2022; Liu et al., 2021; Xu et al., 2023). In the United States, for instance, a sufficiently high CT in the agricultural sector leads to production cost increases of up to 32.6 %; although increases in product prices partially offset this, farmers experience a 11.4–15.5 % decrease in net income (Dumortier and Elobeid, 2021). These examples reveal that very low CT rates may be ineffective, while excessively high rates may threaten economic efficiency (Khastar et al., 2020; Moosavian et al., 2022). Therefore, there is a consensus on the need for a gradual increase in CT rates (Meng and Yu, 2023; Nong et al., 2021). CT not only helps reduce emissions but can also indirectly influence the cost of renewable energy production (Wang et al., 2022). However, the primary effects of environmental policies and carbon pricing appear in the long term, playing a crucial role in achieving sustainable development goals by fostering green innovation (Doğan et al., 2022; Luo et al., 2022; Onwe et al., 2023). In this context, it is projected that energy companies will be forced to develop green finance strategies once CT reaches a certain threshold, thereby creating a nonlinear relationship that promotes the adoption of clean energy plans across the sector (Cheng et al., 2021; Zhu et al., 2020). Therefore, analyzing transition paths to carbon neutrality on a regional and sectoral basis will facilitate the development of urgent action plans (Zhou, 2023).

In conclusion, most of the existing literature primarily focuses on individual energy sources and gives limited attention to holistic analyses that simultaneously consider technical, economic, and environmental aspects of offshore hybrid systems. Particularly, the integration of environmental policy tools such as CT into the optimization processes of these systems has been largely overlooked. However, CT not only accelerates the transformation of energy systems but also directly influences the feasibility of renewable investments. In this context, current research lacks sufficient discussion on how offshore hybrid energy systems can be aligned with carbon-neutral goals and how to balance energy supply security with environmental sustainability. These gaps hinder policymakers, investors, and energy planners from developing forward-looking strategies and act as barriers to realizing green transformation goals. This study's multidimensional analysis approach aims to address this gap by presenting a comprehensive roadmap on how offshore hybrid energy systems can become more efficient, sustainable, and feasible under CT policies. The findings will not only contribute to academic knowledge but also assist governments in shaping green energy incentive mechanisms, analyzing the impacts of environmental tax policies on the energy sector more effectively, and making more holistic decisions in line with long-term carbon neutrality goals.

1.3. Novelty and Contributions

The structure of the study involves the cost optimization of offshore systems, with optimal capacities allocated, and the feasibility outputs are evaluated in detail. Subsequent processes include the effects of carbon taxation on the integration of floating offshore farms, particularly from technical, economic, and environmental perspectives. In this context, there are relatively few credible studies addressing the effects of carbon taxation following optimization procedures for both on-grid and off-grid installations. According to (Zhou et al., 2022), which deals with the integration of battery systems in marine-based cooling processes, the focus is on high costs and the risks of energy losses. (Ghigo et al., 2022), who focused solely on FSPV systems on the island of Lampedusa, performed optimization from a technical and economic perspective. In Irish port facilities, a regional energy cost map was created, considering the wind climate and distance from the shore (Martinez and Iglesias, 2022), while offshore installations were optimized to meet collective energy needs by increasing the share of renewable energy production (Li et al.,

2022a). Referring to the study in the Spanish coast (Vázquez et al., 2024), which claims that solar and wave energy complement each other, a different view is presented in (Ferrari et al., 2020), where the correlation of wind and wave energy in the Mediterranean basin is calculated via an index. In (Lilas et al., 2022), which evaluates offshore installations in seawater reverse osmosis, the focus is on energy management and capacity optimization for electricity and water needs. Compared to the limited body of literature represented by these studies, similar research in the field differs significantly in this regard. This study, where technical, economic, and environmental optimization is achieved through cost minimization, stands apart from (Ghigo et al., 2022) as it considers the integration of wave energy, wind energy, and solar energy. The study also introduces a more innovative framework compared to (Zhou et al., 2022), where marine-based cooling is used, and (Lilas et al., 2022), which focuses on seawater reverse osmosis, since it addresses small-scale microgrid needs in residential, commercial, and industrial areas through on-grid and off-grid hybrid installations. The aim of this study, which involves capacity allocation and feasibility analysis based on cost optimization to meet regional energy needs, differs from (Martinez and Iglesias, 2022) and (Li et al., 2022a), where regional energy cost maps are created. Efforts for energy complementarity are not pursued; instead, the focus is on managing the available energy in the region and integrating battery storage systems based on supply and demand balance, differentiating it from (Vázquez et al., 2024) and (Ferrari et al., 2020). Ultimately, this study focuses on the optimization of a hybrid system that combines floating solar energy systems, OWTs, and wave energy to maximize the use of renewable energy sources in coastal regions. The proposed system optimizes energy production from solar, wind, and wave sources to ensure continuous power generation while minimizing environmental impacts. This research presents a more innovative and sustainable hybrid solution, providing a roadmap for achieving higher energy efficiency and reducing fossil fuel dependence compared to traditional grid-independent systems. Furthermore, this study distinguishes itself by providing an integrated, detailed evaluation of carbon taxation impacts on on-grid offshore hybrid renewable energy systems (HRES), an area that remains underrepresented in current research. While previous works have separately explored hybrid system design, offshore integration, or CT implications, few have comprehensively analyzed their combined techno-economic and environmental effects within an on-grid offshore framework. Here, the influence of varying CT levels on critical economic indicators such as LCOE and net present cost (NPC) is systematically assessed, identifying an optimal CT that balances environmental objectives with economic feasibility. Unlike generalized or location-agnostic models, this research offers a localized and policy-relevant perspective tailored specifically for coastal regions like the Palau River. By doing so, it not only fills an important gap in the literature but also provides practical insights and a strategic roadmap for decision-makers to optimize hybrid energy configurations in the context of evolving carbon taxation policies.

This study is organized as follows: Section 1 presents the motivation, a comprehensive literature review, and the study's key novelties. Section 2 focuses on the materials and methodology related to optimization, including the system's mathematical modeling, assumptions, and case study. Section 3 discusses the optimization results, while Section 4 presents the findings, which are discussed in comparison with credible studies. Finally, Section 5 summarizes the scope, innovations, and findings of the study and offers future research directions based on the final conclusions.

2. MATERIAL AND METHODOLOGY

2.1. System Architecture

2.1.1. Case Areas and Demand Profiles

The Palau River was selected as the case study location due to its

favorable geographic and climatic conditions for offshore HRES. This region exhibits relatively stable solar radiation levels, moderate wave heights, and minimal extreme weather events, which make it a suitable candidate for the deployment of FSPV and other offshore technologies. This area, located in the Southeast Minahasa District of North Sulawesi Province, Indonesia, is used as a case study. The site's geographical coordinates are approximately 1° 03' 43.56" N and 124° 51' 20.27" E. The climate data curve obtained from NASA (NASA, n.d.), based on these coordinates, is presented in Fig. 1.

The solar irradiance and wind speed potentials of the study area are illustrated in thermal maps in Fig. 2(a) and (b), respectively (Global Solar Atlas, n.d.; Global Wind Atlas, n.d.). In Table 1, DNI refers to direct normal irradiation, DHI refers to diffuse horizontal irradiation, and GTI refers to global tilted irradiation. The numerical values in the table also account for ambient temperature to present a comprehensive evaluation of the site's renewable energy potential. (Global Solar Atlas, n.d.; Global Wind Atlas, n.d.). It is important to clarify that the reported value of 1492.1 kWh/kWp refers to the annual specific yield of the FSPV system based on installed capacity, reflecting the actual expected performance of the system. In contrast, the value of 1561.1 kWh/m² corresponds to the theoretical solar resource availability at the site, measured as global horizontal irradiation (GHI). These two values serve different yet complementary purposes: the former is used to assess system-level energy generation, while the latter provides insight into the solar potential of the location.

A demand profile with a daily energy consumption of 500 kWh, a peak power of 70.4 kW, and a load factor of 20 % is considered. The load profile forms a small-scale microgrid consisting of a combination of residential, commercial, and industrial consumers.

2.1.2. System Configuration

An off-grid system is designed to be fully self-sufficient, relying on renewable energy sources such as FSPV, OWT, and wave turbines/tidal generator/wave energy converters (WT/TG/WEC) to meet electricity needs. Energy is stored in batteries for use during periods of insufficient production, such as at night or in adverse weather. In contrast, an on-grid system integrates renewable energy sources with the power grid, utilizing batteries to balance fluctuations in energy production. The system ensures continuous energy flow and provides backup power during grid outages, enhancing reliability and flexibility. Fig. 3 shows the HRES architectures considered in this study. HOMER Pro was utilized in this study to simulate and optimize the performance of a multi-source hybrid energy system. (Fig. 4)

2.1.2.1. Floating Solar Photovoltaic Panel (FSPV). One of the main components of the HRES is the FSPV array. The performance of this module is influenced by several physical and environmental factors, including solar irradiance, panel efficiency, operating temperature, and the module's derating factor (DF), which accounts for real-world losses

such as soiling, shading, and aging. The instantaneous power output of the FSPV array at time t , P_{FSPV}^t , is calculated using Eq. (1), which adjusts the rated capacity P_{FSPV}^{stc} (measured under standard test conditions, STC) by the actual incident solar radiation and temperature effects. This equation can be expressed as:

$$P_{FSPV}^t = P_{FSPV}^{stc} \cdot f_{FSPV} \cdot \frac{IR_t^t}{IR_t^{stc}} \cdot [1 + \alpha_p \cdot (T_C^t - T_C^{stc})], \quad \forall t \quad (1)$$

Here, IR_t^t represents the total solar irradiance incident on the panel at time t , while IR_t^{stc} is the reference irradiance of 1 kW/m² under STC. The factor f_{FSPV} is the DF reflecting performance losses from environmental and operational conditions. The term α_p denotes the temperature coefficient of power (typically negative), reflecting how panel efficiency decreases with increasing cell temperature T_C^t , relative to the reference cell temperature T_C^{stc} (usually 25°C).

The FSPV cell temperature T_C^t at time t is estimated using Eq. (2), which models the thermal behavior of the PV cells based on ambient temperature T_a^t , incident solar radiation G_t^t , and nominal operating cell temperature (NOCT) conditions. This equation captures the heat balance of the cell considering the environmental heat exchange and solar input:

$$T_C^t = \frac{T_a^t + \frac{G_t^t}{G_t^{NOCT}} \cdot (T_C^{NOCT} - T_a^{NOCT}) \cdot \left[1 - \eta_{mp}^{stc} \cdot \frac{1 - \alpha_p \cdot T_C^{stc}}{\tau \cdot \alpha} \right]}{1 + \frac{G_t^t}{G_t^{NOCT}} \cdot (T_C^{NOCT} - T_a^{NOCT}) \cdot \frac{\alpha_p \cdot \eta_{mp}^{stc}}{\tau \cdot \alpha}}, \quad \forall t \quad (2)$$

In this expression, G_t^{NOCT} is the irradiance level (typically 0.8 kW/m²) used to define the NOCT, T_C^{NOCT} and T_a^{NOCT} are the cell and ambient temperatures under NOCT respectively, η_{mp}^{stc} is the maximum power point efficiency at STC, τ is the solar transmittance of any protective cover, and α is the solar absorptance of the PV array. This relationship provides a realistic estimate of cell temperature as it dynamically responds to environmental changes.

Finally, the maximum efficiency of the FSPV panels at STC, η_{mp}^{stc} , is defined by Eq. (3), expressing the ratio of rated power output to the product of irradiated area A_{FSPV} and reference irradiance (IR_t^{stc}):

$$\eta_{mp}^{stc} = \frac{P_{FSPV}^{stc}}{A_{FSPV} \cdot IR_t^{stc}}, \quad \forall t \quad (3)$$

This efficiency metric sets the baseline for performance evaluation under ideal conditions.

All these equations, detailed in the methodology section, are sourced from the HOMER Pro documentation and long-established literature (Demirci et al., 2025; Duffie et al., 2020; Erbs et al., 1982; Graham et al., 1988; Graham and Hollands, 1990; Kazemi-Robati et al., 2024), ensuring their reliability and practical relevance. In response to concerns about methodological transparency, key technical and economic parameters for the FSPV module, such as DF, efficiency, temperature coefficient, and capital/replacement/O&M cost, are clearly presented in Table 2, with references to authoritative sources (C.J. et al., 2024; Goswami et al., 2019; Luo et al., 2021; Rahaman et al., 2023), ensuring clarity and reproducibility. Specifically, the Trina Allmax PD05 flat plate FSPV panel model ("PD05 Panel Datasheet," 2025) was selected, representing a widely used and well-characterized photovoltaic technology.

2.1.2.2. Offshore Wind Turbine (OWT). Wind turbines generate electricity with mechanical power through rotating shafts that rotate the turbines. These turbines can be used in places such as onshore and OWT. Gear losses, generator efficiency, and turbulence effects reduce the actual power output by causing efficiency losses (Li et al., 2022a). The wind speed measured at hub height can vary due to wind shear and other atmospheric conditions, which affect the wind profile at different heights (Khurshid et al., 2024). The wind profile is considered using logarithmic or power-law models, while the turbine operates within a

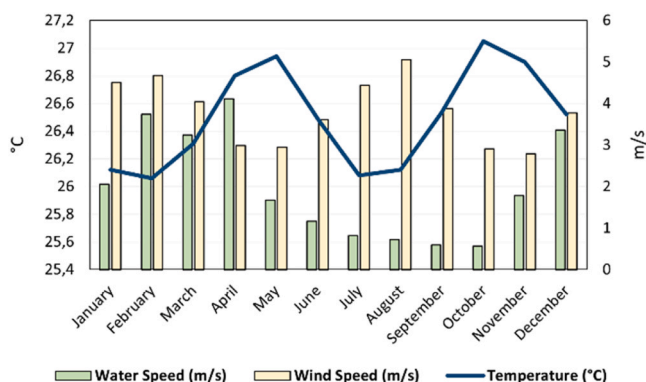


Fig. 1. Geographical climate data of the case area.

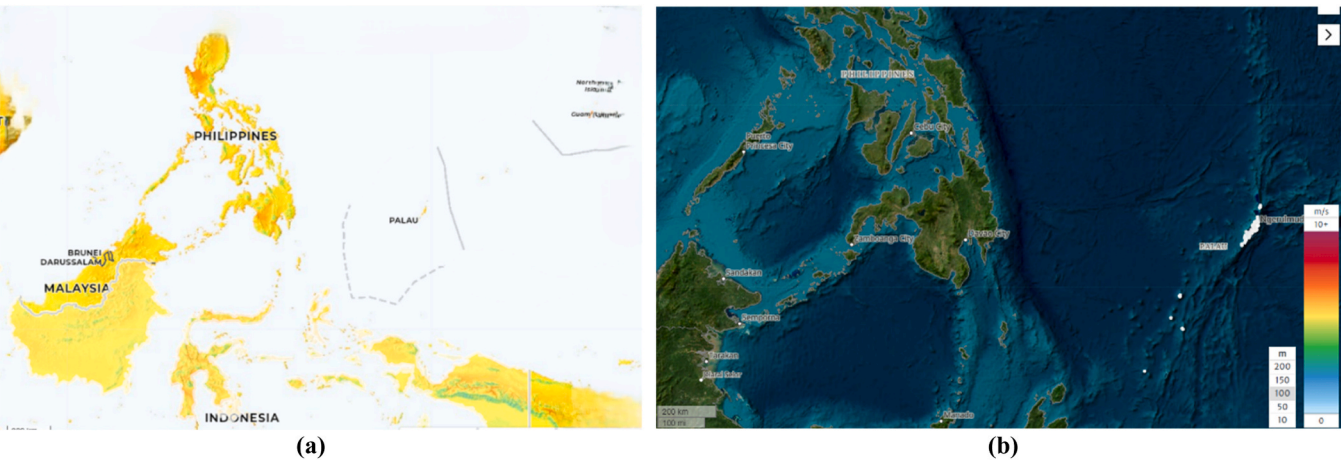


Fig. 2. The potential of solar irradiance (a) and wind speed (b) in the case areas.

Table 1
Geographical data for the case areas.

Parameter	Palau River	Unit	Parameter	Palau River	Unit
Specific FSPV power	1492.1	kWh/kWp	Air temperature	26.9	°C
DNI	1561.1	kWh/m ²	Average wind speed	5.21	m/s
GHI	1859.2	kWh/m ²	Specific WEC power	154	W/m ²
DHI	754.8	kWh/m ²	Anemometer height	100	m
GTI	1879.2	%	Optimum tilt	9 / 180	°

specific range of wind speeds, considering both incoming and outgoing wind speeds (Dash et al., 2023). The OWT output power can vary depending on operating conditions, such as wind speed, turbine settings, and design characteristics, such as blade geometry and pitch control (Khare et al., 2023). Additionally, in OWTs, the platform’s motion introduces an average tilt angle that slightly redirects the rotor away from the incoming wind flow. This aerodynamic misalignment, represented by a tilt angle θ , leads to a reduction in the effective wind speed incident on the rotor and is accounted for in power calculations (Cruz and Atcheson, 2016). To address transparency concerns, the modeling of offshore wind turbines in this study includes detailed formulations for hub-height wind speed estimation (Eq. (4)), which is calculated by HOMER software using the power law, as well as for power output (Eq. (5)) (Markus et al., 2018), air density adjustment (Eq. (6)), and swept area and capacity factor (Eqs. (7–8)) (Petracca et al., 2022), all grounded in well-established aerodynamic and atmospheric principles. All

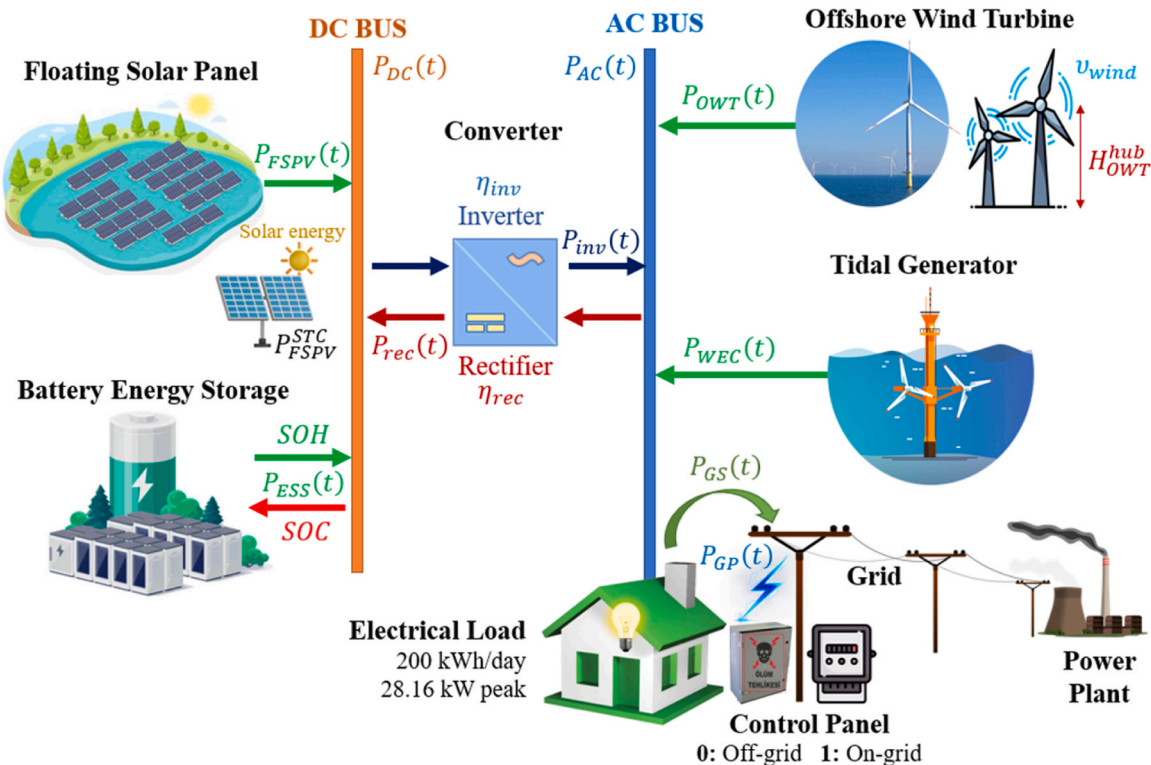


Fig. 3. Hybrid renewable energy system modeling.

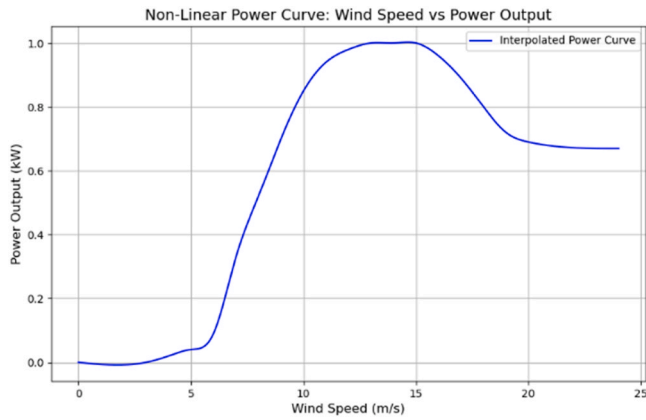


Fig. 4. Offshore wind turbine power curve.

Table 2
FSPV panel technical and economic inputs.

Parameter Name	Value	Unit	Parameter Name	Value	Unit
Derating factor (Jamroen, 2022)	88	%	FSPV capital cost (J. Baptista et al., 2023)	1106	\$/kW
Ground reflectance (Mirzaei et al., 2015)	10	%	FSPV replacement cost (J. Baptista et al., 2023)	1106	\$/kW
Temperature coefficient (Rahaman et al., 2023)	−0.41	%/°C	FSPV O&M cost (J. Baptista et al., 2023)	11.06	\$/kW/yr
Nominal operating cell temperature (C.J. et al., 2024)	44	°C	Lifetime (Goswami et al., 2019)	25.0	yr
Rated capacity	1	kW	Efficiency (Luo et al., 2021)	16.2	%
Cell quantity	60	-	Power output range	250–265	W

technical and economic parameters (Table 3), such as rated capacity, capital cost, and O&M expenses, are clearly disclosed with references (e.g., (Rubio-Domingo and Linares, 2021), enabling full reproducibility. HOMER software considers the power law and calculates the hub height wind speed as in Eq. (4) (“HOMER Pro Manuel Help,” 2025).

Table 3
OWT technical and economic inputs.

Parameter Name	Value	Unit	Parameter Name	Value	Unit
Rated capacity	1	kW	OWT capital cost (Rubio-Domingo and Linares, 2021)	1274	\$/kW
Lifetime	20	year	OWT replacement cost (Rubio-Domingo and Linares, 2021)	1274	\$/kW
Hub height	30	m	OWT O&M cost (Rubio-Domingo and Linares, 2021)	20	\$/kW/yr
Availability losses (Kim et al., 2022)	2–10	%	Performance losses (Sergio Campobasso et al., 2023)	0–2.5	%
Environmental losses (Baas et al., 2023; Malik and Bak, 2025)	7–18	%	Shadowing/wake losses (Pryor and Barthelmie, 2024)	10–35	%
Electrical losses (Lee and Fields, 2021)	1–2	%	Constraint losses (Wikipedia contributors, 2024)	0–2.4	%

$$H_{wind}^{hub} = H_{wind}^{anem} \cdot \left(\frac{H_{OWT}^{hub}}{H_{OWT}^{anem}} \right)^{\varphi} \quad (4)$$

$$P_{OWT}^t = \frac{1}{2} \cdot \rho \cdot A_{OWT} \cdot (v_{wind}^t \cdot \cos(\theta))^3 \cdot C_p(\lambda, \beta), \quad \forall t \quad (5)$$

$$\rho^t = \rho_0 \cdot \frac{P_{OWT}^t}{P_{OWT,STP}^t}, \quad \forall t \quad (6)$$

$$A_{OWT} = \pi \cdot R_{OWT}^2 \quad (7)$$

$$\lambda = \frac{v_{tip}}{v_{wind}} = \frac{\omega \cdot R_{OWT}}{v_{wind}} \quad (8)$$

Here, H_{wind}^{hub} is the wind speed at the hub height of the OWT [m/s], H_{wind}^{anem} is the wind speed at anemometer height [m/s], H_{OWT}^{hub} is the hub height of the OWT [m], H_{OWT}^{anem} is the anemometer height [m], and φ is the power law exponent. Also, P_{OWT}^t is the OWT power output at t time [kW], ρ is actual air density [kg/m^3], ρ_0 is air density at standard temperature and pressure (STP) (1.225 kg/m^3), A_{OWT} is the swept area of the wind turbine rotor, while R_{OWT} is the radius of the wind turbine rotor [m], v_{wind}^t is the wind speed at the height of the turbine rotor at t time [m/s], $C_p(\lambda, \beta)$ is the power coefficient as a function of the tip-speed ratio λ and pitch angle β , which is theoretically 0.593, β is the angle at which the blades are adjusted relative to the wind direction [°], v_{tip} represents the speed of the blade tip [m/s], while ω is the rotational speed of the turbine in radians per second.

In HOMER, the cost of a maintenance event is calculated as the sum of a fixed cost and the marginal cost multiplied by the number of turbines. For instance, a fixed dispatch cost of 100 \$ may represent the baseline cost for deploying personnel to the site, while a marginal cost of 500 \$ per turbine (e.g., for oil replacement) results in a total cost of 2600 \$ for five turbines. However, in this study, it is assumed that maintenance will not be performed at regular intervals. Therefore, parameters related to maintenance, such as procedure, interval, type, downtime, and marginal cost, are not considered in the analysis. However, an alternative aspect concerning turbine performance-related losses is considered within the scope of this study, and the relevant details can be found in Table 3. In this study, the main types of losses considered include: availability losses, which correspond to downtime due to failures or maintenance activities (Wilkie and Galasso, 2020); performance losses, resulting from aerodynamic inefficiencies, control strategy limitations, or mechanical wear (DNV GL, 2022); environmental losses, arising from the corrosive nature of the marine environment, salt accumulation, and biofouling effects that reduce turbine efficiency (Canning, 2019); shadowing losses, caused by aerodynamic interference between closely spaced turbines (Donglin et al., 2023); electrical losses, which occur due to resistance and conversion inefficiencies in the power transmission infrastructure (Pryor and Barthelmie, 2024); and constraint losses, stemming from grid flexibility limitations, transmission bottlenecks, or regulatory restrictions that prevent turbines from operating at full capacity (Wikipedia contributors, 2024). All these loss categories are considered in energy yield estimations and economic evaluations to ensure realistic modeling of system behavior.

2.1.2.3. Tidal Energy or Wave Energy Converters (WECs). The annual tidal potential energy can be calculated using the tidal range for consecutive rising and falling tides for each time step, as shown in Eq. (9) (Chowdhury et al., 2021).

$$E_{WEC} = \sum_{i=1}^n \left(\frac{1}{2} \cdot \rho_T \cdot g \cdot H_i^2 \right) \quad (9)$$

Here, i represents each consecutive rising and falling tide in a year ($n \approx 1411$), H_i is the tidal range (water head difference) [m], ρ_T refers to the density of seawater, g represents the acceleration due to gravity [m/

s^2], while the global potential energy density is summarized in Fig. 5. Another important aspect is the calculation of the power output of the water turbine's generator at t time (P_{WEC}^t) in Eqs. (10)–(11). For more details, refer to (Neill et al., 2018).

$$P_{WEC}^t = \rho_T \cdot g \cdot Q_T^t \cdot H \cdot \alpha_T, \quad \forall t \quad (10)$$

$$Q_T^t = C_D \cdot A_s \cdot \sqrt{2gH^t}, \quad \forall t \quad (11)$$

Here, Q_T^t denotes the turbine flow rate, α_T represents a general efficiency factor associated with the turbines, C_D is a discharge coefficient, and A_s is the cross-sectional flow area [m^2]. The power curve of the hydrokinetic turbine shows the relationship between water speed [m/s] and power output [kW]. The power output starts to increase significantly from a water speed of 2 m/s and reaches a peak of approximately 3.5 kW at 4 m/s (Fig. 6). At higher water speeds, the power remains constant. This indicates the maximum efficiency limit of the turbine in converting kinetic energy into electricity. These data provide important insights into the system's performance, highlighting that it is designed to harness energy from currents with high efficiency (Li et al., 2022b).

The technical and economic parameters of WEC are as shown in Table 4. In this system, Poseide 66 River and Marine Current Turbine model was preferred (GUINARD Energies, 2017). The model parameters, including seawater density, tidal range, turbine discharge coefficient, and generator efficiency, are explicitly stated, enhancing the model's reproducibility and aligning with the standards of transparent techno-economic analysis.

2.1.2.4. Converter or Power Conversion System (PCS). To supply standard electrical loads, the DC electricity produced by FSPV modules must be converted into AC. This conversion is a crucial aspect of system performance. As such, a converter has been incorporated into the system design. The converter power output calculations are given Eqs. (12)–(13) (HOMER Energy, n.d.).

$$P_{inv}^t = \eta_{inv} \cdot P_{DC}^t, \quad \forall t \quad (12)$$

$$P_{rec}^t = \eta_{rec} \cdot P_{AC}^t, \quad \forall t \quad (13)$$

Here, the inverter (P_{inv}^t) and rectifier (P_{rec}^t) power output at time t [kW] determine the powers to be supplied by the converter. η_{inv} and η_{rec} are shown the inverter and rectifier efficiency [%], respectively. In this system, the converter lifetime is 15 years, capital and replacement costs are 300 $\$/kW$, and the O&M cost is 5 $\$/kW/yr$ (Al Saadi and Ghosh, 2024; Atallah et al., 2020). The converter, serving both as an inverter and a rectifier, operates with an efficiency of 95 % for both modes, assuming a relative efficiency of 100 %.

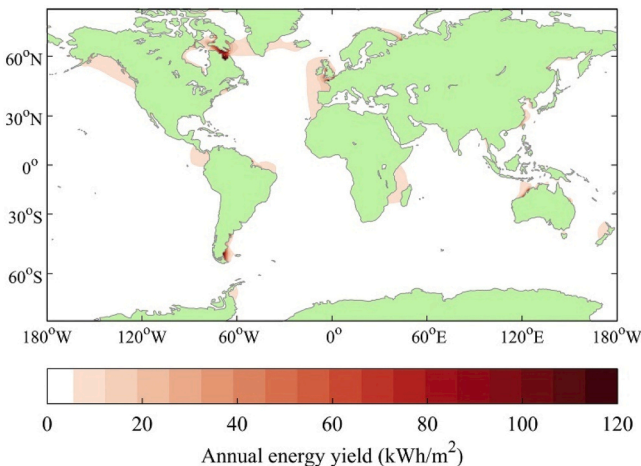


Fig. 5. The global theoretical tidal range energy resource.

2.1.2.5. Battery Energy Storage System (ESS). The effective functioning of the HRES relies heavily on the proper allocation of the ESS for efficiently storing clipped energy (CE). The energy output of the ESS depends on its charging and discharging conditions, which are determined by the state of energy (SoE_{ESS}^t). The energy state of the ESS is computed using Eq. (14), factoring in both the charging and discharging efficiencies (η_{chr} and η_{disch}) and the corresponding power inputs ($P_{ESS,chr}^t$ and $P_{ESS,disch}^t$), along with its energy state from the previous time step (SoE_{ESS}^{t-1}) (Choi et al., 2021). Furthermore, as described in Eq. (15), the ESS's aging process restricts its energy state to a range between 20 % and 100 % (Terkes et al., 2024b).

$$SoE_{ESS}^t = SoE_{ESS}^{t-1} + P_{ESS,chr}^t \cdot \eta_{chr} - \frac{P_{ESS,disch}^t}{\eta_{disch}}, \quad \forall t \quad (14)$$

$$SoE_{ESS}^{max} \geq SoE_{ESS}^t \geq SoE_{ESS}^{min}, \quad \forall t \quad (15)$$

A fresh battery-based ESS is modeled using a modified lithium battery (ASM) approach. Four distinct sub-models, derived from the Arrhenius equation, have been developed to account for the following factors: overall functionality, temperature and relative capacity, depth of discharge (DoD)-dependent cycle life, and temperature-dependent shelf life. The power loss and theoretical capacity are determined using Eqs. (16) and (17) (Terkes et al., 2024a). In this context, P_{ESS}^{thr} denotes the output or throughput power of the ESS, while V_0 , R_0 , and I represent the nominal voltage, series resistance, and current of the ESS, respectively. The current corresponding to the maximum ESS output power is indicated by $I_{P_{thr}}^{max}$.

$$P_{ESS}^{thr} = V_0 I - R_0 I^2 \quad (16)$$

$$I_{P_{thr}}^{max} = \frac{V_0}{2R_0} \quad (17)$$

The temperature-dependent capacity can be calculated using the temperature and battery characteristics, which are defined by the constants d_0 , d_1 , and d_2 , as shown in Eq. (18) (Manwell and McGowan, 1993). The cycle degradation curves for each DoD can either be obtained from the battery manufacturer or calculated using Eqs. (19) and (20) (ASTM, 2023). Even when the ESS is not actively in use, capacity loss may still occur due to temperature-based calendar degradation. The aging effect, modeled using the Arrhenius equation, is described in Eq. (21) (Smith et al., 2012). In this context, the ESS capacity corresponding to the available temperature is denoted as $C_{ESS}^{T_{avail}}$, whereas under nominal temperature conditions, it is represented as $C_{ESS}^{T_{nom}}$. The parameters of the capacity curve are d_0 , d_1 , and d_2 , with T representing the available ESS temperature. The variable A denotes the DoD coefficient, DoD^β corresponds to the DoD exponent fitting, and N refers to the project year. Additionally, D represents the exponential coefficient accounting for degradation due to time and temperature, while k_t is the constant representing the storage rate (h^{-1}).

$$C_{ESS}^{T_{avail}} = C_{ESS}^{T_{nom}} \cdot (d_0 + d_1 T + d_2 T^2) \quad (18)$$

$$\frac{1}{N} = A \cdot DoD^\beta \quad (19)$$

$$D = \sum_{i=0}^N A \cdot D_i^\beta \quad (20)$$

$$k_t = B \cdot e^{-\frac{d}{T}} \quad (21)$$

The maximum charging and discharging power of the ESS is computed at each timestep. The charging power determines whether excess renewable electricity can be stored. These powers vary with each timestep based on the state of charge (SoC). Three distinct constraints are applied to the ESS's maximum charging power. The first constraint,

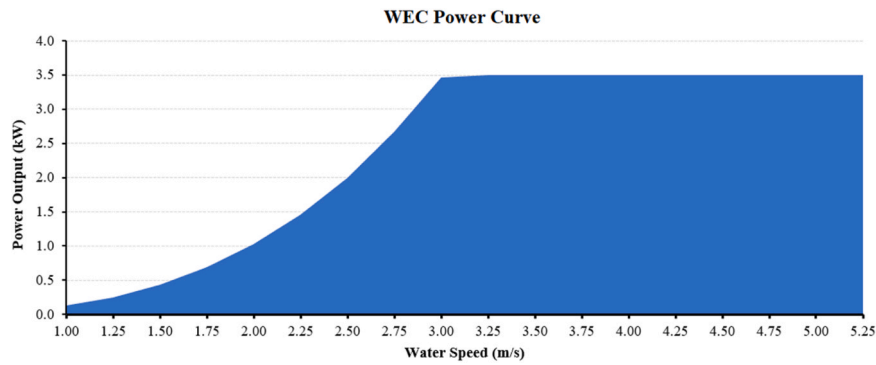


Fig. 6. P66 turbine power curve.

Table 4

WEC technical and economic inputs.

Parameter Name	Value	Unit	Parameter Name	Value	Unit
Rated capacity	3.5	kW	Turbine speed (nominal)	2.5	m/s
Size (area)	1 m x 1.5 m	m ²	Turbine power continuous output	2	kW
Weight	80	kg	WEC capital cost (Abdullah et al., 2021; Majdi Nasab et al., 2021; Toumi et al., 2023)	4025	\$/kW
Rotor diameter	660	Nm	WEC replacement cost (Abdullah et al., 2021; Majdi Nasab et al., 2021; Toumi et al., 2023)	3500	\$/kW
Water depth required	1.5	m	WEC O&M cost (Abdullah et al., 2021; Majdi Nasab et al., 2021; Toumi et al., 2023)	201.25	\$/kW/yr
Seawater density (Fofonoff and Millard, 1983)	~1025	kg/m ³	Turbine discharge coefficient (Engineering Toolbox, 2024)	0.6–0.85	-
Tidal range (NOAA, 2025)	0.3–1.5	m	Generator efficiency (Logan, 1981)	90–95	%

based on the kinetic battery model, defines the maximum discharge power ($P_{c_{max,kbm}}^{ESS}$) as given in Eq. (22). The second constraint, which considers the maximum C-rate, is calculated by Eq. (23) and denoted as $P_{c_{max,mcr}}^{ESS}$. The third constraint pertains to the ESS's maximum charging current and is determined by Eq. (24), represented as $P_{c_{max,mcc}}^{ESS}$. Finally, the actual maximum charging power $P_{c_{max}}^{ESS}$ is obtained by minimizing among these three constraints, as defined in Eq. (25). Additionally, the maximum discharge power for a given operation period $P_{d_{max,kbm}}^{ESS}$ is calculated using Eq. (26), and the maximum useful discharge power $P_{d_{max}}^{ESS}$ is determined by Eq. (27) (Terkes et al., 2023).

$$P_{c_{max,kbm}}^{ESS} = \frac{k \cdot Q_{avail}^{ESS} \cdot e^{-k \cdot \Delta t} + Q_{init}^{ESS} \cdot k \cdot c \cdot (1 - e^{-k \cdot \Delta t})}{1 - e^{-k \cdot \Delta t} + c \cdot (k \cdot \Delta t - 1 + e^{-k \cdot \Delta t})} \quad (22)$$

$$P_{c_{max,mcr}}^{ESS} = \frac{(1 - e^{-a_c \Delta t}) \cdot (Q_{max}^{ESS} - Q_{init}^{ESS})}{\Delta t} \quad (23)$$

$$P_{c_{max,mcc}}^{ESS} = \frac{N_{bat} \cdot I_{max} \cdot V_0}{1000} \quad (24)$$

$$P_{c_{max}}^{ESS} = \frac{\min(P_{c_{max,kbm}}^{ESS}, P_{c_{max,mcr}}^{ESS}, P_{c_{max,mcc}}^{ESS})}{\sqrt{\eta_{rt}^{ESS}}} \quad (25)$$

$$P_{d_{max,kbm}}^{ESS} = \frac{-k \cdot c \cdot Q_{max}^{ESS} + k \cdot Q_{avail}^{ESS} \cdot e^{-k \cdot \Delta t} + Q_{init}^{ESS} \cdot k \cdot c \cdot (1 - e^{-k \cdot \Delta t})}{1 - e^{-k \cdot \Delta t} + c \cdot (k \cdot \Delta t - 1 + e^{-k \cdot \Delta t})} \quad (26)$$

$$P_{d_{max}}^{ESS} = \sqrt{\eta_{rt}^{ESS}} \cdot P_{d_{max,kbm}}^{ESS} \quad (27)$$

Here k is the ESS rate constant [1/hr], Q_{init}^{ESS} is the available energy at the beginning of the t time step [kWh], Δt is the time step [hr], Q_{avail}^{ESS} is the total amount of energy at the end of the t time step [kWh], Q_{max}^{ESS} is the total storage capacity [kWh], c is the ESS capacity ratio, a_c represents the maximum charge rate of the storage system (in A/Ah). N_{bat} denotes the total number of batteries in the storage system, while I_{max} refers to the peak charging current of the storage (in A). V_0 indicates the nominal voltage of the storage system, and η_{rt}^{ESS} represents the round-trip efficiency of the battery system (in %). Finally, the technical parameters of the ESS mathematical model are explained in Table 5 (Terkes et al., 2023), while Table 6 presents the technical and economic parameters of the ESS (Fofang and Tanyi, 2020; Ramesh and Saini, 2020). In this system, the Enphase AC lithium iron phosphate (LFP) model was

Table 5

Technical parameters for fresh battery pack.

Parameters	Fresh Battery (FB)
Useful capacity (kWh)	1
State of health (%)	100
Nominal voltage (V)	3.7
Maximum charge current (A)	270
Maximum discharge current (A)	810
Maximum capacity (Ah)	270.27
Rate constant (1/hr)	79.29
Capacity ratio	1
Effective series resistance (mΩ)	0.36049
Maximum operating temperature (°C)	50
Minimum operating temperature (°C)	0
Other round-trip losses (%)	8
Initial state of charge (%)	100
Minimum state of charge (%)	20
Degradation limit (%)	50
End of life (EoL)	
Calculate EoL by	Calendar or cycling degradation, whichever is greater
Cycling degradation uses DoD based on	Degraded battery capacity
Curve Parameters	
Relative capacity vs. temperature	d ₀ : 0.923, d ₁ : 0.00345, d ₂ : -0.0000375
DoD vs. cycles to failure	A: 0.00014423, β: 1.7945
Shelf-life vs. temperature	B: 1.267, d: 3826.70644

Table 6
Energy storage technical and economic inputs.

Parameter Name	Value	Unit	Parameter Name	Value	Unit
Capacity (kWh)	1.2	kWh	ESS capital cost (Terkes et al., 2024c)	300	\$/kWh
Capacity (Ah)	48.5	Ah	ESS replacement cost (Terkes et al., 2024c)	300	\$/kWh
Nominal capacity (Ah)	5	Ah	ESS O&M cost (Terkes et al., 2024c)	5	\$/kWh/yr
Initial SoC	100	%	Rated output power	270	VA
Minimum SoC	20	%	Duration of discharge at rated power	4.3	hr
Degradation ratio	50	%	Nominal voltage	25.6	VDC
Roundtrip cell efficiency	93.4	%	Charge current (max.)	1.13	A
Ambient operating temperature (min.)	−20	°C	Discharge current (max.)	1.13	A
Ambient operating temperature (max.)	45	°C	Lifetime	10	yr

preferred (Enphase Energy, 2017).

2.1.3. Assumptions and Other Considerations

In designing the hybrid energy system, several key assumptions and assessments were made to ensure optimal performance and financial sustainability. These assumptions are particularly important in evaluating the feasibility and long-term viability of the system within the context of Indonesia's renewable energy landscape. Electricity purchase and sale prices from the grid are critical factors for the project's profitability. In Indonesia, there is a two-tiered electricity purchasing tariff from the grid. Between 17.00 and 22.00, the purchase price (C_{TOT}^t) is 0.07 \$/kWh, while during low-demand periods (22.00–17.00), the price is 0.05 \$/kWh. Electricity sold to the grid (C_{sale}^t) is priced at 0.0914 \$/kWh during peak hours (17.00–22.00) and 0.0653 \$/kWh during off-peak hours (22.00–17.00) (PT PLN (Persero), n.d.). The price differences create an opportunity to purchase electricity during low-demand periods and sell at higher prices during peak demand, generating profit. To evaluate the financial sustainability of energy projects, important parameters such as inflation and discount rates are considered. The inflation rate (f) is set at 1.71 % (Bank Indonesia, n.d.), and the discount rate (i) is 6.25 % (Bank Indonesia, n.d.). The project lifespan (N) is assumed to be 25 years, allowing for comprehensive financial analysis and the development of strategies to ensure long-term success. The environmental impact of grid electricity is also considered during the design process. It is assumed that each 1 kWh of electricity purchased from the grid results in 800 g of CO₂ in Indonesia. Similarly, carbon monoxide emissions are 100 g/kWh, and particulate matter is 0.20 g/kWh. Sulfur dioxide and nitrogen dioxide emissions are 1.50 g/kWh and 0.60 g/kWh, respectively (Minister of Energy and Mineral Resources of the Republic of Indonesia, 2015).

2.2. Scenarios

In this study, several scenarios are considered to analyze the impact of different configurations of the HRES model and CT rates on the overall system performance. The specific CT rates selected for scenarios C through F (20, 40, 60, and 80 \$/tCO₂) are based on a comprehensive review of current and projected international carbon pricing frameworks and policies. These values reflect the range of CT implementations observed globally, from emerging markets with lower CT rates to advanced economies with more aggressive carbon pricing strategies

aimed at achieving net-zero emissions by mid-century (International Energy Agency, 2023). For instance, CTs in European countries currently range between approximately 20–100 \$/tCO₂, with some nations planning gradual increases aligned with their Nationally Determined Contributions (NDCs) under the Paris Agreement (Baranzini et al., 2017; Organisation for Economic Co-operation and Development (OECD), 2023; World Bank, 2024). The lower bound scenario (20 \$/tCO₂) represents initial implementation stages, whereas the higher bound (80 \$/tCO₂) reflects more stringent climate policies anticipated in the near future. By incorporating this spectrum of CT values, the study captures the economic impacts of a variety of policy environments, enhancing the generalizability and practical relevance of the findings. Moreover, the selected CT rates enable an assessment of how incremental increases in carbon pricing influence system economics, such as operational costs, payback periods, and investment attractiveness. This approach aligns with ongoing trends in environmental policy that aim to internalize the social costs of carbon emissions, thereby incentivizing renewable energy adoption and discouraging fossil fuel dependency. Thus, these scenarios provide critical insights for policymakers and investors considering the financial and environmental trade-offs under different regulatory conditions.

Fig. 7 shows the HRES model flowchart. The purpose of these scenarios is to assess how varying levels of grid reliance and carbon taxation influence the economic feasibility and sustainability of the proposed system. The analysis will help determine the optimal conditions under which the system operates efficiently, ensuring rapid payback, high renewable energy utilization, and minimal excess electricity generation. The scenarios include both grid-dependent and off-grid HRES with varying CT rates. These scenarios allow for a comprehensive evaluation of the system's performance under different regulatory and operational conditions. Also, the effect of increasing CTs on the system's economic feasibility is analyzed. CTs are varied in the scenarios to assess how external environmental policies could influence the financial viability of the system. The objective of these scenarios is to provide a detailed analysis of the system's behavior and performance across different settings, which will guide decision-making regarding the most feasible and sustainable solution for energy generation.

Table 7 contains a brief summary of the scenarios carefully evaluated in this study.

2.3. Feasibility Assessment and Performance Metrics

The NPC is the difference between the present value of a system's costs and revenues over its lifetime. NPC is a crucial financial indicator that considers the time value of money by discounting all costs and cash flows to their present value. This allows for the assessment of the long-term financial viability of energy projects. It is HOMER's main economic output, used to rank system configurations and calculate the annualized cost and LCOE. On the other hand, LCOE is defined as the average cost per kWh of useful electrical energy produced by the system. HOMER calculates the annualized cost of electricity production by subtracting the cost of serving the thermal load from the total annualized cost and then dividing it by the total electric load served, and this gives the system's cost per unit of electrical load served. While the LCOE is a useful metric for comparing different systems, HOMER does not use it as a basis for ranking system configurations. LCOE provides a measure of the total cost incurred for producing a unit of energy, facilitating a comparison of the cost-effectiveness of different energy technologies, particularly in the context of renewable energy projects. For the calculation of economic performance indicators, the real interest rate is initially obtained using the nominal interest rate and inflation rate as shown in Eq. (28). The annualized costs, including investment, O&M, replacement, CT, grid purchase (GP), and grid sale (GS), are calculated respectively using Eqs. (29) to (34). The LCOE is then determined based on the total annualized cost obtained from Eq. (35), as given in Eq. (36). The capital recovery factor (CRF) is calculated according to Eq. (37) and

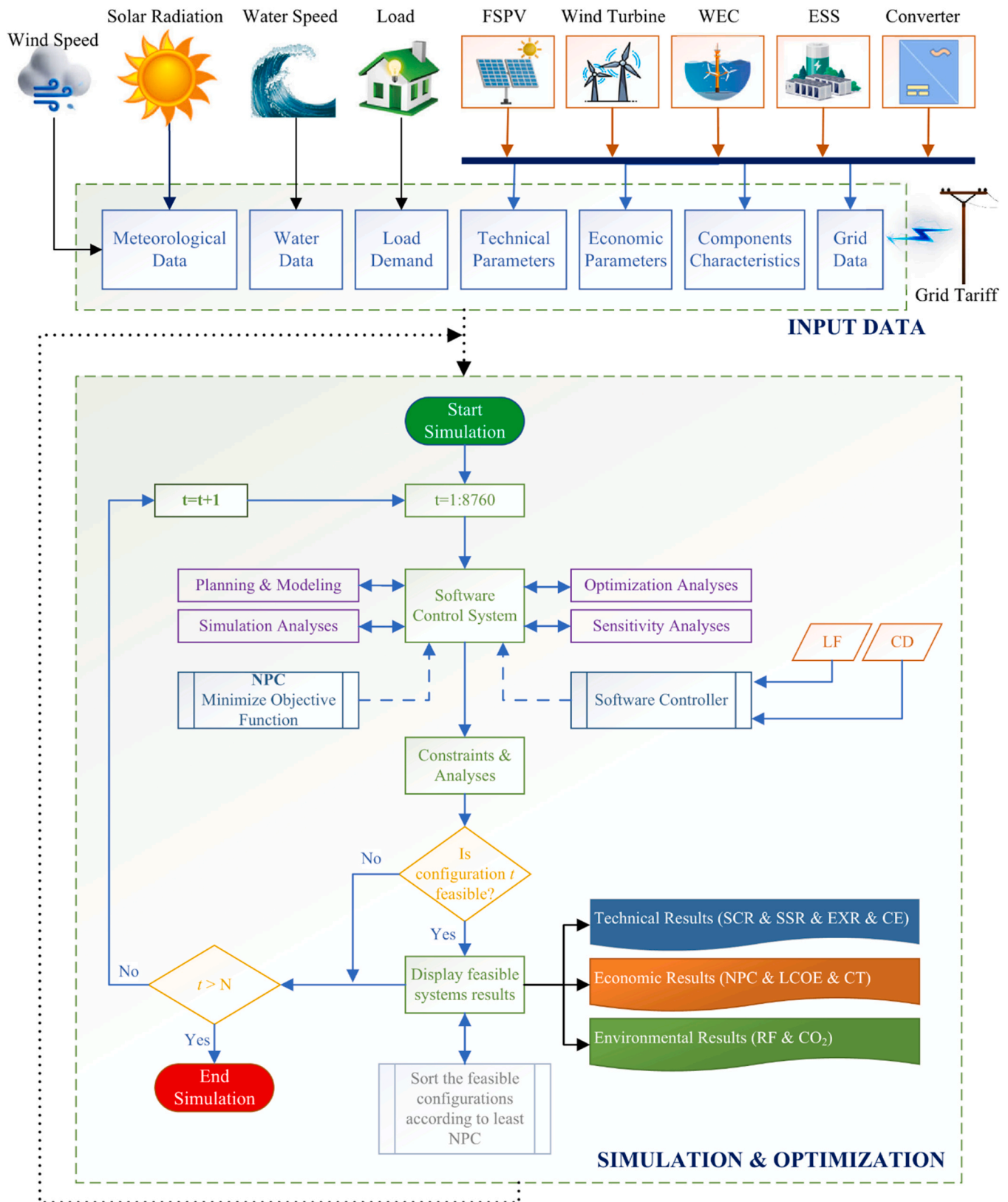


Fig. 7. HRES flowchart.

used in the NPC calculation presented in Eq. (38). The CRF is used to convert a present value into a series of equivalent annual payments over the lifetime of an asset. It facilitates the calculation of annualized costs, allowing for consistent comparison and evaluation of investment

expenses across different project durations. Overall, the objective function of the optimization is the minimization of NPC. All equations presented in this study are sourced from All the equations used herein are derived from the study by (Terkes et al., 2023).

Table 7
Scenarios.

Scenarios	On-Grid HRES	Off-Grid HRES	CT (\$/tCO ₂)
A	-	✓	-
B	✓	-	0
C	✓	-	20
D	✓	-	40
E	✓	-	60
F	✓	-	80

$$i = \frac{i - f}{1 + f} \quad [\%] \quad (28)$$

$$C_{inv}^{ann} = C_{inv}^{FSPV} + C_{inv}^{OWT} + C_{inv}^{WEC} + C_{inv}^{ESS} + C_{inv}^{con} \quad [\$ / yr] \quad (29)$$

$$C_{O\&M}^{ann} = C_{O\&M}^{FSPV} + C_{O\&M}^{OWT} + C_{O\&M}^{WEC} + C_{O\&M}^{ESS} + C_{O\&M}^{con} \quad [\$ / yr] \quad (30)$$

$$C_{rep}^{ann} = C_{rep}^{FSPV} + C_{rep}^{OWT} + C_{rep}^{WEC} + C_{rep}^{ESS} + C_{rep}^{con} \quad [\$ / yr] \quad (31)$$

$$C_{tax}^{ann} = TCO_2 \cdot CO_2^{tax} \quad [\$ / yr] \quad (32)$$

$$C_{GP}^{ann} = \sum_{t=0}^{8760} (P_{GP}^t \cdot C_{ToU}^t), \quad \forall t \quad [\$ / yr] \quad (33)$$

$$C_{GS}^{ann} = \sum_{t=0}^{8760} (P_{GS}^t \cdot C_{sale}^t), \quad \forall t \quad [\$ / yr] \quad (34)$$

$$C_{total}^{ann} = C_{inv}^{ann} + C_{O\&M}^{ann} + C_{rep}^{ann} + C_{tax}^{ann} + C_{GP}^{ann} - C_{GS}^{ann} - C_{salvage}^{ann} \quad [\$ / yr] \quad (35)$$

$$LCOE = \frac{C_{total}^{ann}}{\int P_L \cdot dt} \quad [\$ / kWh] \quad (36)$$

$$CRF_{i,N} = \frac{i \cdot (1+i)^N}{(1+i)^N - 1}, \quad \forall i, N \quad (37)$$

$$Minimize \left(C_{NPC} = \frac{C_{total}^{ann}}{CRF_{i,N}} \right), \quad \forall i, N \quad [\$] \quad (38)$$

Here, C_{total}^{ann} is the annualized total cost [\$/yr], and $\int P_L \cdot dt$ is the amount of electricity supplied to the load [kWh]. Also, $CRF_{i,N}$ is capital recovery factor, i is an annual real interest rate [%], i is nominal interest rate [%], f is the expected inflation rate [%], N is project lifetime [yr], C_{inv}^{ann} is initial investment cost [\$/yr], $C_{O\&M}^{ann}$ is total maintenance cost [\$/yr], C_{rep}^{ann} is average annual replacement cost [\$/yr], C_{tax}^{ann} is total CT [\$/yr], C_{GP}^{ann} is total cost of purchasing electricity [\$/yr], C_{GS}^{ann} is revenue from selling electricity [\$/yr], CO_2^{tax} is CT [\$/tCO₂], TCO_2 is annual CO₂ [t/yr], P_{GP}^t is the electricity purchased from the grid at t time [kW], P_{GS}^t is the electricity sold to the grid at t time [kW], C_{ToU}^t is cost of electricity purchased at t time [\$/yr], and C_{sale}^t is the revenue from selling electricity at t time [\$/yr]. In these calculations, the total discounted and annualized cost is represented by a specific term, and the amount of electricity provided to the load is another key factor. The total cost for each year, denoted by this term, includes all relevant expenses such as installation, operations, maintenance, and storage costs. The discount rate is also incorporated, as well as the project lifespan, which is measured in years.

In investment analysis, two widely used methods are the simple payback (SP) and discounted payback (DP) approaches. The SP method provides a quick estimate of the time required to amortize the initial investment, while the DP method accounts for the time value of money, offering a more precise evaluation by factoring in the discount rate. The payback period refers to the number of years in which all costs injected into the project will be recovered. The calculations for SP and DP are

carried out using Eq. (39) (Ozturk et al., 2024), respectively.

$$SP = \frac{C_{inv}^{ann}}{C_{total}^{ann}}; DP = \frac{C_{inv}^{ann}}{C_{NPC}} \quad [yr] \quad (39)$$

Alternatively, important performance indicators include the self-supply ratio (SSR), which represents the percentage of energy demand satisfied by on-site energy production. The self-consumption rate (SCR) reflects the proportion of generated energy directly consumed within the system, while the renewable fraction (RF) indicates the share of total energy production from renewable sources, highlighting the project's commitment to environmental sustainability. In calculating these three parameters related to renewable energy and environmental performance, the value of $\int P_{HRES} \cdot dt$ must first be considered. This value represents the total power produced at time steps t by the FSPV, OWT, and WEC systems, obtained through integration (see Eq. (40)). Besides P_{HRES} , the variables P_F and P_G are also considered in the calculations. Here, P_F represents the difference between the hybrid system's energy production (P_{HRES}) and the combined demand of the ESS power and load power when the system's production exceeds the load demand at time t ($P_F^t = P_{HRES}^t - P_L^t - P_{ESS}^t$). Conversely, P_G denotes the difference between the load power demand and the combined output of the hybrid system's total power and ESS power when the load demand exceeds the hybrid system's production at time t ($P_G^t = P_L^t - P_{HRES}^t - P_{ESS}^t$). Using these definitions, the SCR, SSR, and RF values can be calculated with the help of Eqs. (41)–(43). In the calculations of P_F and P_G , factors such as electricity sold to the grid (P_{GS}), electricity purchased from the grid (P_{GP}), curtailed electricity due to grid feed-in limits ($P_{curtail}$) that cannot be utilized by the load, and total losses resulting from ESS charge-discharge cycles and converter inverter/rectifier operations (P_{loss}) are also consider. For detailed formulations of all these equations, refer to (Terkes et al., 2024a) and (Demirci et al., 2025).

$$\int P_{HRES} \cdot dt = \int P_{FSPV} \cdot dt + \int P_{OWT} \cdot dt + \int P_{WEC} \cdot dt \quad (40)$$

$$SCR = \left(\frac{\int P_{HRES} \cdot dt - \int P_F \cdot dt}{\int P_{HRES} \cdot dt} \right) \cdot 100 \quad [\%] \quad (41)$$

$$SSR = \left(\frac{\int P_{HRES} \cdot dt - \int P_G \cdot dt}{\int P_L \cdot dt} \right) \cdot 100 \quad [\%] \quad (42)$$

$$RF = \left(\frac{\int P_{HRES} \cdot dt - \int P_G \cdot dt - \int P_F \cdot dt}{\int P_{HRES} \cdot dt + \int P_G \cdot dt} \right) \cdot 100 \quad [\%] \quad (43)$$

CE represents the portion of energy produced by the hybrid system that cannot be utilized or is wasted due to the limitations of the grid's capacity. This parameter is calculated using Eq. (44) (Terkes et al., 2023), where the total energy production of the system at a given time is represented by one term, and the grid or demand capacity limit is denoted by another. Another important metric is the energy exchange rate (EXR), which is calculated by subtracting the energy supplied from renewable sources to meet the load from the total demand, then dividing the result by the total load. The EXR essentially indicates the reduction in grid dependence and is computed based on Eq. (45) (Terkes et al., 2023).

$$CE = \left(\frac{\int P_{curtail} \cdot dt}{\int P_{HRES} \cdot dt - \int P_G \cdot dt} \right) \cdot 100 \quad [\%] \quad (44)$$

$$EXR = \left(\frac{\int P_L \cdot dt - \int P_G \cdot dt}{\int P_L \cdot dt} \right) \cdot 100 \quad [\%] \quad (45)$$

3. OPTIMIZATION RESULTS

The optimization and feasibility results are evaluated in three distinct subsections. First, the off-grid-based hybrid system to be

installed offshore is examined, followed by the on-grid operational scenario. Within the on-grid-based results, outcomes under different CT scenarios are presented individually. A comparative evaluation of the shared optimization results is provided in the final section (Discussion). In this context, while comparing the off-grid and on-grid configurations of such a HRES intended for offshore installation, the significant effects of CT on key feasibility metrics are carefully analyzed. The proposed optimal CT level for the system to be deployed at the Palau River, along with its potential benefits, is expected to serve as guidance for researchers and relevant stakeholders. To assess the optimization results, the optimal system capacities that yield the minimum cost are first presented. Economic performance is evaluated using metrics such as NPC, LCOE, SP, and DP. Meanwhile, self-consumption and environmental performance are quantified via RF, SCR, SSR, EXR, and CO₂ emissions. For proper system sizing, it is desirable to minimize CE and thus reduce waste in electricity production. Accordingly, relevant metric results are also included. The feasibility outcomes for both the off-grid and on-grid HRES configurations are summarized in Table 8.

3.1. Off-Grid Feasibility Results (Scenario A)

The off-grid feasibility results for the Palau River hybrid system indicate promising outcomes. The system, comprising a total FSPV capacity of 241 kW, an OWT capacity of 10.5 kW (three units rated at 3.5 kW each), and a WT/TG/WEC capacity of 17.5 kW, achieves a 100 % renewable fraction, ensuring full reliance on clean energy sources. The LCOE is 2.51 \$/kWh, indicating a competitive cost for energy production, while the NPC stands at 682.29 k\$, reflecting the total investment required. Notable performance metrics include an SCR of 31.16 % and a high SSR of 83.2 %, demonstrating efficient utilization of the generated energy. Furthermore, the system operates with zero CO₂ emissions, highlighting its strong environmental sustainability. These results confirm the system's technical and economic feasibility, featuring minimal energy waste and a negligible environmental footprint, thereby positioning it as a highly effective off-grid solution for the Palau River. The detailed feasibility results for the off-grid system are presented in Table 8.

3.2. On-Grid Feasibility Results (Scenario B-C-D)

The feasibility results for Scenarios B, C, and D are presented in Table 8. The on-grid HRES feasibility analysis for Palau River under these scenarios reveals key insights. Scenario B, which does not incorporate a CT, yields an LCOE of 0.01697 \$/kWh and an NPC of 114.38 k\$, indicating a highly cost-effective configuration. The system achieves a RF of 80.4 % and limits CO₂ emissions to 70.91 tons/yr. With the integration

of CTs in Scenarios C and D, the LCOE increases to 0.02011 \$/kWh and 0.0211 \$/kWh, respectively. Despite the rise in costs, the system maintains a SCR of approximately 25.92 % and a SSR of 51.78 %, reflecting a reasonable degree of energy independence. Furthermore, both scenarios continue to offer substantial reductions in carbon emissions. These findings highlight the trade-off between CT-induced cost impacts and environmental performance, with the system maintaining high RF levels and contributing to significant emissions reductions.

3.3. On-Grid Feasibility Results (Scenario E)

The on-grid feasibility results for Scenario E, which includes a CT of 60 \$/tCO₂, illustrate the system's sensitivity to higher carbon pricing. The system records an LCOE of 0.02672 \$/kWh and an NPC of 180.61 k\$, reflecting increased costs relative to previous scenarios. Despite the higher CT, the system maintains a RF of 80.9 % and continues to deliver notable environmental benefits, with CO₂ emissions reduced to 69.35 tons/yr. The SCR stands at 26.1 %, while the SSR reaches 52.86 %, indicating efficient utilization of locally generated energy. An EXR of 52.5 % demonstrates a substantial decrease in grid dependency and reflects the system's effectiveness in balancing generation and consumption. Overall, although the CT raises costs, the system remains economically feasible and environmentally robust. The corresponding feasibility results for Scenario E are summarized in Table 8.

3.4. On-Grid Feasibility Results (Scenario F)

The on-grid feasibility results for Scenario F, with a CT of 80 \$/tCO₂, reflect a further shift towards renewable energy. The LCOE is 0.0226 \$/kWh, and the NPC is 177.31 k\$, indicating a moderate increase in costs with the higher CT. The system achieves a high RF of 90.2 %, demonstrating a strong reliance on renewable sources. The SCR is 27.24 %, while the SSR increases significantly to 71.91 %, highlighting the system's efficient use of the generated energy. Additionally, the system maintains a low environmental impact, with carbon emissions of just 41.22 tons/yr. Overall, the higher CT in Scenario F enhances the system's renewable output, improving its sustainability and reducing its carbon footprint. These results are presented in Table 8.

4. DISCUSSIONS

This section presents a comprehensive analysis divided into five key parts. First, the comparative feasibility of off-grid and on-grid systems under Scenario B is examined, highlighting their respective advantages and limitations for offshore HRES installations. Second, the effects of the CT on system performance and economic viability are evaluated in

Table 8
Feasibility results for HRES Scenarios.

Specifications	Off-grid	On-grid					Units
	Scenario A	Scenario B	Scenario C	Scenario D	Scenario E	Scenario F	
Carbon tax	-	-	20	40	60	80	\$/tCO ₂
FSPV	241	-	-	-	2.61	67.3	kW
OWT	3	1	1	1	3	2	units
WT/TG/WEC	17.5	105	105	105	105	105	kW
ESS	581	-	-	-	3.67	1.20	kWh
PCS	74.8	-	-	-	-	51.3	kW
NPC	682.29	114.4	135.5	135.5	180.6	177.3	k\$
LCOE	2.51	0.017	0.020	0.020	0.027	0.023	\$/kWh
CE	60.0	0.1	0.1	0.1	0.4	0.07	%
SP	9.17	8.03	7.32	7.32	6.41	7.29	yr
DP	9.23	10.19	9.06	9.06	7.72	9.01	yr
SCR	31.16	25.92	25.92	25.92	26.10	27.24	%
SSR	83.2	51.78	51.78	51.78	52.86	71.91	%
EXR	83.2	51.43	51.43	51.43	52.50	71.76	%
RF	100	80.40	80.40	80.40	80.90	90.2	%
CO ₂	-	70.91	70.91	70.91	69.35	41.22	t/yr

detail. Third, the proposed optimal CT value is introduced, offering practical guidance for policymakers aiming to balance environmental goals with cost-effectiveness. Fourth, the implications of the energy supply chain within the hybrid system are discussed, emphasizing operational challenges and integration strategies. Finally, the socio-economic impacts and workforce dynamics associated with offshore hybrid systems are analyzed to provide a holistic understanding of their broader effects on the community and industry stakeholders.

4.1. Off-Grid vs. On-Grid (Scenarios B)

A detailed comparative analysis between the off-grid and on-grid HRES configurations reveals substantial differences in both economic and technical performance. The most prominent distinction is observed in the LCOE, which is significantly higher in the off-grid system (2.51 \$/kWh) compared to the on-grid configuration (0.01697 \$/kWh). This stark contrast is primarily attributable to the absence of grid support in the off-grid model, necessitating oversizing of both energy generation (particularly PV capacity) and storage components to ensure uninterrupted power supply. The high upfront capital cost of the battery energy storage system, along with replacement and maintenance costs over the project lifetime, significantly inflates the overall NPC, which stands at 682.29 k\$ for the off-grid setup. In contrast, the grid-connected system benefits from grid electricity as a backup, thus allowing a more cost-efficient system architecture with reduced battery and PV oversizing, yielding a much lower NPC of 114.38 k\$, corresponding to an 83.2 % cost reduction.

From a performance standpoint, the off-grid HRES demonstrates superior sustainability metrics, achieving 100 % RF, 60.4 % higher SSR, and 20 % higher SCR compared to the on-grid model. Moreover, the off-grid system generates zero carbon emissions, while the on-grid counterpart is responsible for approximately 70.91 tons of CO₂ per year, due to its partial reliance on grid electricity, which is not entirely derived from renewable sources.

However, these environmental advantages come at the cost of economic feasibility. The exorbitant LCOE of the off-grid model makes it less attractive for widespread adoption, particularly in regions where grid access is available and reliable. The cost differential is rooted not only in the scale of infrastructure required but also in the limited operational flexibility and higher risk of unmet load during extended low irradiance periods, which necessitates further storage or generation redundancy.

While the off-grid system ensures full autonomy and environmental benefits, the on-grid model offers a more economically viable pathway with moderate compromise on renewable penetration. These trade-offs are visually depicted in the comparative feasibility analysis presented in Fig. 8, guiding policymakers and stakeholders toward selecting the most appropriate configuration based on regional priorities, infrastructure availability, and environmental regulations.

4.2. Carbon Tax (CT) Effects

When comparing the effects of the CT between Scenario B (0 \$/tCO₂) and Scenario F (80 \$/tCO₂), several key differences are observed. The LCOE increases by 33.2 %, from 0.01697 \$/kWh in Scenario B to 0.0226 \$/kWh in Scenario F. Similarly, the NPC rises by 55.1 %, from 114.38 k\$ to 177.31 k\$, reflecting the added economic burden of higher CT. In terms of performance, the SCR increases slightly by 5.1 % in Scenario F, while the SSR improves significantly by 39 %. EXR also increases by 39.5 % in Scenario F. RF improves by 11.2 % in Scenario F, reaching 90.2 % compared to 80.4 % in Scenario B, while the environmental benefit is more significant (41.9 % reduction) in Scenario F. Overall, the higher CT in Scenario F leads to increased renewable energy adoption and lower carbon emissions, though it also results in higher costs and a larger proportion of excess energy. Also, the feasibility results for Scenarios B–F are presented in Fig. 8.

These findings align with several studies in the literature that examine the role of carbon taxation in shaping hybrid renewable system design and performance (Table 9). For instance, the cost increase observed in Scenario F under an 80 \$/tCO₂ tax is consistent with outcomes reported by (Flórez-Orrego et al., 2021; Gabbar and Esteves, 2023), where systems incorporating carbon capture or advanced hybridization only became economically favorable above tax thresholds of 60 \$/tCO₂. Similarly, the substantial reduction in CO₂ (41.9 %) under higher CT pressure mirrors the results in (Zhang et al., 2022), where emission reductions of up to 49 % were achieved through the inclusion of offshore energy hubs when the CT exceeded 100 €/tCO₂. The upward shift in system cost indicators, such as the 55.1 % increase in NPC and 33.2 % increase in LCOE observed in Scenario F, also finds support in (Cranmer and Baker, 2020), where high CT scenarios significantly enhanced the climate value of offshore wind contributions. Furthermore, improvements in system reliability and self-sufficiency indicators (RF, SSR, EXR) under a higher carbon price, as noted in the present study, are in line with results from (Iqbar et al., 2022; Schetinger et al., 2025), where carbon pricing incentivized the deployment of hybrid renewable solutions with greater technical and economic resilience. (Yang et al., 2022; Yuksel et al., 2024) additionally highlight the long-term economic competitiveness of low-emission systems, such as nuclear and floating renewable platforms, under stringent CT regimes, supporting the conclusion that high carbon pricing mechanisms can drive a shift toward low-carbon infrastructure despite increased initial investment requirements. The present study's results, particularly the enhanced renewable fraction and environmental performance under elevated CT levels, reinforce this pattern. Lastly, findings from (Niyiul and Koirala, 2024; Sabine et al., 2020) underscore the importance of coupling CT policies with complementary regulatory frameworks and reinvestment strategies. This complements the economic trade-offs highlighted in Scenario F, where higher taxation not only curtails emissions but also necessitates greater upfront investment and system oversizing, evidenced by increased excess energy. Therefore, the current results corroborate the broader literature, indicating that while carbon taxation imposes economic burdens, it also effectively incentivizes cleaner and more resilient energy architectures when paired with appropriate planning and support mechanisms.

4.3. Proposed Optimal Carbon Tax (CT)

The effects of CT up to 40 \$/tCO₂ on the feasibility results exhibit similar trends. Gradually increasing the CT may help identify the most beneficial rate that induces significant changes in system performance. Accordingly, the CT was adjusted in increments of 1 \$/tCO₂ between 40 \$/tCO₂ and 60 \$/tCO₂, and the feasibility results were reassessed. The similar feasibility results up to a 40 \$/tCO₂ CT remained almost unchanged, even with a CT of 53 \$/tCO₂. The notable effects of the CT, especially with a 54 \$/tCO₂ policy, are promising for the offshore hybrid system to be installed at Palau River. Therefore, the initial CT for researchers and relevant stakeholders seeking to deploy such systems should be set at 54 \$/tCO₂. Guiding future efforts in this direction, together with advanced engineering solutions, can transform sustainable communities and urban systems into achievable realities, fostering environmental awareness and self-sufficiency.

4.4. Energy Supply Chain Implications

The deployment of offshore HRES, integrating FSPV, OWTs, and WECs, introduces complex challenges and dependencies across the energy supply chain (Gatzert and Kosub, 2016). While the present study primarily addresses techno-economic optimization and environmental impacts, an in-depth consideration of supply chain vulnerabilities and resilience is imperative for robust system design and sustainable operation.

Energy supply chains underpinning offshore renewable installations

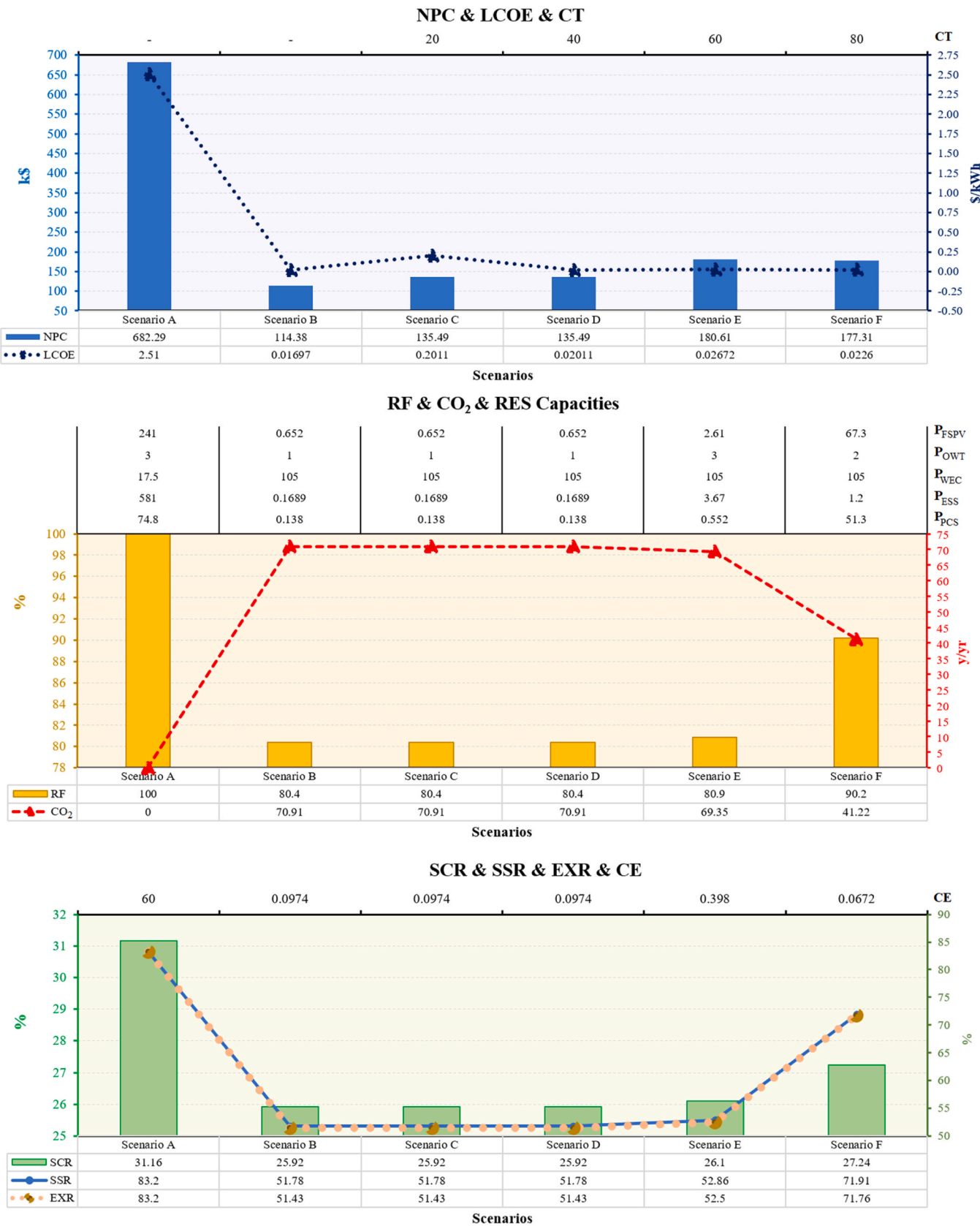


Fig. 8. Feasibility comparison results graphics.

Table 9
Comparative overview of carbon tax (CT) influence in renewable energy planning.

Ref.	CT (\$/tCO ₂)	System & Location	Method/Model	Economic Result	CT Effect
(Cranmer and Baker, 2020)	60–100	Grid + OWT + ESS, US coastal regions	Global change assessment model	Offshore wind reduces abatement costs, 100–450 B\$ climate value.	High CT (100 \$/tCO ₂) boosts offshore wind climate benefits.
(Zhang et al., 2022)	55–500 €/t	Grid + FSPV + OWT + ESS, Norwegian North Sea	A multi-period mixed-integer linear programming (MILP) model	Offshore energy hubs (OEHs) improve flexibility and cut losses, aiding decarbonization.	≥ 100 €/tCO ₂ favors hydrogen production, cuts emissions up to 49 %.
(Schetinger et al., 2025)	10–50	OWT + ESS, Santos Basin, Brazil	HOMER Pro	Wind shares 30–70 % yield best financial results.	> 40 \$/tCO ₂ enables hybrids to outperform conventional systems.
(He et al., 2022)	60–180 RMB	Grid + OWT, Chinese coastal province	Financial life cycle pricing	Electricity price adjusted to 0.514 RMB/kWh, carbon revenue offsets investment.	Carbon market revenues lower costs, increase competitiveness.
(Sabine et al., 2020)	100 €/t	FSPV + Biomass + Hydro, Réunion Island	Computable general equilibrium (CGE) model (GetRun-NRJ)	CT negatively impacts GDP.	Using tax revenues socially/ environmentally improves acceptance.
(Flórez-Orrego et al., 2021)	0–100	OWT + cogeneration + power plant, ultra-deep waters	Thermoflow®, Aspen, Monte Carlo	40 % of investment cost reduced by time delays.	> 60 \$/tCO ₂ CT makes carbon capture and reinjection (CCS) systems financially positive.
(DiLellio et al., 2025)	44 GMB/MWh	Grid + OWT + WEC, UK	LCOE, internal rate of return (IRR), sustained cost of energy (SCOE)	IRR favors short-term payback; SCOE better for long-term.	CT helps shift investments to low/ zero carbon tech.
(Yang et al., 2022)	24.39 & 150	Floating nuclear power plant (FNPP) + OWT + FSPV, Russia & Japan	Cost-benefit analysis	FNPP lowest energy cost due to reliability & low fuel (130 \$/tU).	100 \$/tCO ₂ CT makes electric ships cheaper than fuel ships.
(Gabbar and Esteves, 2023)	5–50	Grid + FSPV + OWT + small modular reactors (SMRs) (NRHES), Jakarta, Indonesia	HOMER Pro	18 % NPC reduction, 11.6 % IRR, 7.4 yrs payback.	50 \$/tCO ₂ tax makes fossil generation economically inferior to NRHES.
(Yuksel et al., 2024)	100 & 250 €/t	Organic Rankine cycle (ORC)-based waste heat recovery system (WHRS) + FNPP, Dominican Republic	A Python-based simulation framework and TOPSIS	Nuclear’s economic success depends on LCOE.	Nuclear gains long-term edge due to zero operational CO ₂ .
(Iqbar et al., 2022)	26.1	OWT + gas turbine generator (GTG), Malaysia	Theoretical modeling, Weibull distribution, life cycle cost model	Hybrid system LCOE 22 % lower than conventional.	CT input strengthens hybrid system’s economic edge.
(Nyiwul and Koirala, 2024)	0–100	FSPV + OWT, Africa (SA, Morocco, etc.)	A statistical modeling approach using patent data and policy performance indices	Financial support alone insufficient to overcome barriers.	Legal and transparent carbon pricing needed to boost effectiveness.
(Flórez-Orrego et al., 2022)	0–100	Floating production storage and offloading (FPSO) platforms, ultra-deep offshore waters	Thermoflow®, Aspen®, MATLAB® tools	Without CT, CCS costly; with 40–100 \$/tCO ₂ & low rates, high NPV & IRR.	Low or zero CT makes CCS financially unattractive.
This Study	0–80	Grid + FSPV + OWT + WEC + ESS, Palau River in Indonesia	HOMER Pro	CT reduces grid-connected system costs by 15–22 %.	A 54 \$/tCO ₂ CT optimally balances policy and system factors like battery degradation and inverter efficiency.

are inherently exposed to multifaceted risks, including raw material scarcity (notably critical minerals for photovoltaic cells and wind turbine components), manufacturing bottlenecks, transportation constraints, and logistical disruptions exacerbated by offshore site remoteness (Chou et al., 2021; Leimeister and Kolios, 2018). According to (Zhao et al., 2023), these factors significantly increase operational risks and introduce temporal and financial uncertainties in project execution and maintenance.

Moreover, CT regimes, by internalizing environmental externalities, modulate cost drivers along the supply chain, incentivizing the optimization of sourcing strategies to minimize carbon-intensive processes (Babagolzadeh et al., 2020). This economic signal can catalyze supply chain reconfiguration towards localized manufacturing hubs (Luo et al., 2022; Wang et al., 2017), enhanced circular economy practices (Hariga et al., 2017), and adoption of advanced digital supply chain management tools (Manupati et al., 2020; Zhang et al., 2024), such as block-chain for provenance tracking (Abiodun et al., 2025; Esmaeilian et al., 2020) and AI-driven demand forecasting (Wang et al., 2025).

Therefore, future offshore hybrid energy system designs should incorporate comprehensive supply chain risk assessment models that capture material flow constraints, geopolitical factors, and environmental impacts (Khan, 2025; Smith, 2023). Integrating such models with techno-economic optimization frameworks will allow for a holistic evaluation of system feasibility, incorporating not only LCOE and NPC

but also supply chain robustness and adaptability metrics.

Such multidisciplinary approaches are critical to ensure that the ambitious carbon reduction targets facilitated by offshore renewables are not undermined by supply chain fragility, thus securing both economic viability and long-term operational resilience in the face of evolving global challenges.

4.5. Socio-Economic Implications and Workforce Dynamics in Offshore Hybrid Systems

In addition to techno-economic indicators such as NPC and LCOE, a comprehensive evaluation of offshore HRES necessitates the inclusion of socio-economic dimensions, particularly employment generation, regional development potential, and societal integration. These factors play a pivotal role in determining the long-term sustainability and public acceptance of such systems.

From a systems engineering perspective, the deployment of FSPV, OWTs, and WECs requires a multidisciplinary labor force across various project stages, including civil and electrical engineering, maritime logistics, structural assembly, and systems integration (Clark et al., 2023). During the construction phase, offshore hybrid systems can yield high labor intensity, while the O&M phase offers stable, long-term employment opportunities, especially in coastal communities with pre-existing maritime infrastructure (Fan et al., 2025; Lüth and Keles, 2024).

Moreover, localized manufacturing and supply chain activities, such as the fabrication of floating platforms, turbine blades, anchoring systems, and control units, can catalyze regional industrial diversification (Mäkitie et al., 2018; Zhang et al., 2019). When aligned with targeted policy incentives and workforce development programs, offshore hybrid projects can serve as economic multipliers, stimulating green jobs and innovation hubs in marine technology sectors.

Recent studies have emphasized the importance of quantifying employment factors within renewable energy optimization models (Ding et al., 2023; IRENA and ILO, 2022). Integrating these metrics into cost-based simulations enables a more holistic understanding of energy system feasibility, balancing technical efficiency with socio-economic value creation.

In the context of this study, although the optimization primarily centers around LCOE and NPC, future extensions should explore employment elasticity with respect to system capacity, regional labor specialization, and supply chain localization. Such integrative modeling approaches can support policymakers in designing hybrid energy strategies that are not only cost-optimal but also socially inclusive and economically regenerative, particularly in coastal zones that stand to benefit from the decentralization of clean energy infrastructures.

5. CONCLUSION

This study rigorously evaluated the techno-economic and environmental feasibility of an offshore HRES deployed at Palau River, under various CT scenarios and grid configurations. The findings elucidate the critical balance between economic viability and environmental sustainability, demonstrating that while off-grid HRES achieves complete renewable penetration, its elevated LCOE and NPC pose substantial financial challenges. Conversely, on-grid configurations under progressive CT regimes manifest notable improvements in renewable energy share, carbon emissions reduction, and system reliability, albeit with increased upfront and operational costs.

From a technical perspective, the analysis highlights the significant influence of CT levels on dispatch strategies and battery storage utilization, emphasizing the need for adaptive control algorithms that optimize energy flows dynamically in response to both economic signals and weather variability. The identification of \$4 /tCO₂ as an optimal CT threshold further underscores the interplay between policy design and system technical parameters, such as battery degradation rates and inverter efficiency, which directly affect long-term system performance and cost-effectiveness.

Furthermore, the study advocates for integrating advanced forecasting models, including machine learning-based solar irradiance and load predictions, to enhance system operation by reducing reliance on conservative reserve margins and thus lowering overall system costs. Future research can adopt a comparative methodology evaluating different machine learning algorithms, such as LSTM, XGBoost, and Transformer-based models, for short-term solar and load forecasting under offshore environmental conditions. These models can be tested using real-time sensor data integrated into digital twin frameworks to simulate operational outcomes. The potential inclusion of hybrid energy storage systems, combining battery technologies with thermal or hydrogen storage, is proposed to improve temporal load balancing and extend system lifespan through diversified cycling patterns. To validate this hybrid storage configuration, experimental testbeds or pilot-scale prototypes using modular battery-thermal integration can be deployed, where cycling profiles, degradation behaviors, and energy dispatch strategies are monitored under controlled offshore simulation environments.

Future research should also explore the impact of grid-connected offshore hybrid systems on ancillary services, such as frequency regulation and reactive power support, leveraging smart inverter functionalities and demand response schemes to provide grid stability and maximize renewable penetration. In this context, real-time Hardware-

in-the-Loop (HIL) simulations and power hardware emulation setups can be employed to evaluate inverter-grid interaction dynamics and assess the technical feasibility of providing fast-frequency response in offshore grid conditions. Incorporating real-time health monitoring and predictive maintenance techniques can further optimize operational expenditures and mitigate unplanned outages, contributing to higher system availability. As a methodological extension, condition-based monitoring systems using machine learning classifiers trained on sensor data (e.g., vibration, temperature, voltage trends) can be developed and validated through offshore pilot installations, enabling predictive analytics tailored for marine environments.

Practically, the results support the formulation of dynamic policy instruments, such as time-variant carbon pricing and performance-based subsidies, which incentivize deployment of technically optimized offshore hybrid systems. Moreover, fostering regional industrial capacities in component manufacturing, installation, and maintenance is essential for ensuring scalability and sustainable economic growth.

In summary, this work not only bridges the gap between technical modeling and policy assessment but also sets a foundation for multidisciplinary strategies that couple advanced energy system design with forward-looking regulatory frameworks. Such integrative approaches are vital for accelerating the transition towards low-carbon, resilient offshore energy infrastructures capable of meeting future climate and energy security objectives.

CRedit authorship contribution statement

Musa Terkes: Validation, Resources, Writing – review & editing, Software, Formal analysis, Writing – original draft, Supervision, Methodology. **Muhammad Rizqi Asy Syarif:** Writing – original draft, Conceptualization, Software, Visualization, Methodology. **Alpaslan Demirci:** Writing – review & editing, Supervision, Visualization, Conceptualization, Validation, Methodology. **Zafer Ozturk:** Writing – original draft, Conceptualization, Visualization. **Erdin Gokalp:** Writing – review & editing, Methodology, Supervision. **Umit Cali:** Writing – review & editing, Supervision, Validation, Conceptualization, Methodology.

Declaration of Competing Interest

The authors declare that they have no known competing financial interests or personal relationships that could have appeared to influence the work reported in this paper.

Data availability

The authors are unable or have chosen not to specify which data has been used.

References

- Abdullah, C., Mad Kaidi, H., Sarip, S., Shafie, N., 2021. Small scale standalone solar and tidal hybrid power system in isolated area. *Renew. Energy Focus* 39, 59–71. <https://doi.org/10.1016/j.ref.2021.07.010>.
- Abiodun, T.P., Nwulu, N.I., Olukanmi, P.O., 2025. Application of Blockchain Technology in Carbon Trading Market: A Systematic Review. *IEEE Access* 13, 5446–5470. <https://doi.org/10.1109/ACCESS.2024.3523672>.
- Abrell, J., Kosch, M., Rausch, S., 2022. How effective is carbon pricing?—A machine learning approach to policy evaluation. *J. Environ. Econ. Manag.* 112, 102589. <https://doi.org/10.1016/j.jeem.2021.102589>.
- Ahmadi, Y., Yamazaki, A., Kabore, P., 2022. How Do Carbon Taxes Affect Emissions? Plant-Level Evidence from Manufacturing. *Environ. Resour. Econ.* 82, 285–325. <https://doi.org/10.1007/s10640-022-00678-x>.
- Al Saadi, K., Ghosh, A., 2024. Investigating the integration of floating photovoltaics (FPV) technology with hydrogen (H₂) energy for electricity production for domestic application in Oman. *Int. J. Hydrog. Energy* 80, 1151–1163. <https://doi.org/10.1016/j.ijhydene.2024.07.260>.
- Alcañiz, A., Monaco, N., Isabella, O., Ziar, H., 2024. Offshore floating PV–DC and AC yield analysis considering wave effects. *Energy Convers. Manag.* 300, 117897. <https://doi.org/10.1016/j.enconman.2023.117897>.

- Alex, A., Petrone, R., Tala-Ighil, B., Bozalakov, D., Vandevelde, L., Gualous, H., 2022. Optimal techno-enviro-economic analysis of a hybrid grid connected tidal-wind-hydrogen energy system. *Int. J. Hydrog. Energy* 47, 36448–36464. <https://doi.org/10.1016/j.ijhydene.2022.08.214>.
- ASTM, 2023. Practices for Cycle Counting in Fatigue Analysis. ASTM Int. <https://doi.org/10.1520/E1049-85R23>.
- Atallah, M.O., Farahat, M.A., Lotfy, M.E., Senjyu, T., 2020. Operation of conventional and unconventional energy sources to drive a reverse osmosis desalination plant in Sinai Peninsula, Egypt. *Renew. Energy* 145, 141–152. <https://doi.org/10.1016/j.renene.2019.05.138>.
- Baas, P., Verzijlbergh, R., van Dorp, P., Jonker, H., 2023. Investigating energy production and wake losses of multi-gigawatt offshore wind farms with atmospheric large-eddy simulation. *Wind Energy Sci.* 8, 787–805. <https://doi.org/10.5194/wes-8-787-2023>.
- Babagolzadeh, M., Shrestha, A., Abbasi, B., Zhang, Y., Woodhead, A., Zhang, A., 2020. Sustainable cold supply chain management under demand uncertainty and carbon tax regulation. *Transp. Res. Part D. Transp. Environ.* 80, 102245. <https://doi.org/10.1016/j.trd.2020.102245>.
- Bahadori, M., Ghassemi, H., Bahadori, M.S., 2019. Feasibility study of hybrid offshore wind turbine with solar platform in Persian Gulf. *Adv. Renew. Energies Offshore - Proc. 3rd Int. Conf. Renew. Energies Offshore, RENEW 2018* 797–802.
- Balta, H., Yumurtaci, Z., 2024. Investigation and Optimization of Integrated Electricity Generation from Wind, Wave, and Solar Energy Sources. *Energies* 17. <https://doi.org/10.3390/en17030603>.
- Bank Indonesia, n.d. Discount Rate in Indonesia [WWW Document]. CNN Indones. URL (<https://www.cnnindonesia.com/ekonomi/20240620143120-78-1111953/bi-tahan-suku-bunga-di-625-persen-pada-juni-2024>) (accessed 10.21.24b).
- Bank Indonesia, n.d. Inflation Rate in Indonesia [WWW Document]. Cent. Bur. Stat. URL (<https://www.bps.go.id/id/presreleaset/2024/11/01/2309/inflasi-year-on-year-y-on-y-pada-oktober-2024-sebesar-1-71-persen-inflasi-provinsi-y-on-y-tertinggi-terjadi-di-provinsi-papua-tengah-sebesar-4-19-persen.html>) (accessed 10.21.24a).
- Baptista, J., Vargas, P., Ferreira, J.R., 2023. Positive effects of the migration from Ka-band satellite to 4G solution for the communication needs of a scattered set of 1 MW solar farms in Poland: A user's experience. *REPQJ* 19. <https://doi.org/10.24084/repqj19.214>.
- Baranzini, A., van den Bergh, J.C.J.M., Carattini, S., Howarth, R.B., Padilla, E., Roca, J., 2017. Carbon pricing in climate policy: seven reasons, complementary instruments, and political economy considerations. *Wiley Interdiscip. Rev. Clim. Chang* 8.
- Benjamins, S., Williamson, B., Billing, S.-L., Yuan, Z., Collu, M., Fox, C., Hobbs, L., Masden, E.A., Cottier-Cook, E.J., Wilson, B., 2024. Potential environmental impacts of floating solar photovoltaic systems. *Renew. Sustain. Energy Rev.* 199, 114463. <https://doi.org/10.1016/j.rser.2024.114463>.
- Bi, C., Law, A.W.-K., 2023. Co-locating offshore wind and floating solar farms – Effect of high wind and wave conditions on solar power performance. *Energy* 266, 126437. <https://doi.org/10.1016/j.energy.2022.126437>.
- C.J., R., Lim, K.H., Kurnia, J.C., Roy, S., Bora, B.J., Medhi, B.J., 2024. Design study on the parameters influencing the performance of floating solar PV. *Renew. Energy* 223, 120064. <https://doi.org/10.1016/j.renene.2024.120064>.
- Canning, C., 2019. The University of Edinburgh. *Corros. Biofouling Offshore Wind Monopile Found.*
- Cheng, Y., Sinha, A., Ghosh, V., Sengupta, T., Luo, H., 2021. Carbon tax and energy innovation at crossroads of carbon neutrality: Designing a sustainable decarbonization policy. *J. Environ. Manag.* 294, 112957. <https://doi.org/10.1016/j.jenvman.2021.112957>.
- Cho, S., Kim, J., Lim, D., 2024. Optimal design of renewable energy certificate multipliers using an LCOE-Integrated AHP model: A case study of South Korea. *Renew. Energy* 226, 120386. <https://doi.org/10.1016/j.renene.2024.120386>.
- Choi, Y.J., Oh, B.C., Acquah, M.A., Kim, D.M., Kim, S.Y., 2021. Optimal operation of a hybrid power system as an island microgrid in south-korea. *Sustain* 13, 1–18. <https://doi.org/10.3390/su13095022>.
- Chou, J.-S., Liao, P.-C., Yeh, C.-D., 2021. Risk Analysis and Management of Construction and Operations in Offshore Wind Power Project. *Sustainability* 13. <https://doi.org/10.3390/su13137473>.
- Chowdhury, M.S., Rahman, K.S., Selvanathan, V., Nuthammachot, N., Suklueng, M., Mostafaeipour, A., Habib, A., Akhtaruzzaman, M., Amin, N., Techato, K., 2021. Current trends and prospects of tidal energy technology. *Environ. Dev. Sustain* 23, 8179–8194. <https://doi.org/10.1007/s10668-020-01013-4>.
- Clark, C., McDowell, B., Stefek, J. (ORCID:0000000339105494), 2023. Offshore Wind Workforce Safety Standards and Training Resource. United States.
- Colasante, A., D'Adamo, I., Morone, P., 2022. What drives the solar energy transition? The effect of policies, incentives and behavior in a cross-country comparison. *Energy Res. Soc. Sci.* 85, 102405. <https://doi.org/10.1016/j.erss.2021.102405>.
- Cranmer, A., Baker, E., 2020. The global climate value of offshore wind energy. *Environ. Res. Lett.* 15, 54003. <https://doi.org/10.1088/1748-9326/ab7667>.
- Cruz, J., Atcheson, M., 2016. *Floating offshore wind energy: the next generation of wind energy*. Springer.
- Dash, R.L., Mohanty, B., Hota, P.K., 2023. Energy, economic and environmental (3E) evaluation of a hybrid wind/biodiesel generator/tidal energy system using different energy storage devices for sustainable power supply to an Indian archipelago. *Renew. Energy Focus* 44, 357–372. <https://doi.org/10.1016/j.ref.2023.01.004>.
- Demirci, A., Ozturk, Z., Terkes, M., Mirza Tercan, S., Yumurtaci, R., Cali, U., 2025. Can Electric Vehicle Charging Stations Be Carbon Neutral With Solar Renewables? *IEEE Access* 13, 9739–9754. <https://doi.org/10.1109/ACCESS.2025.3526736>.
- DiLellio, J., Aggidis, G., Vandercruyssen, D., Howard, D., 2025. Economic Methods for the Selection of Renewable Energy Sources: A Case Study. *Sustainability* 17. <https://doi.org/10.3390/su17114857>.
- Ding, K., Zhang, L., Yang, C., Wang, Z., 2023. The optimization analysis of multi-type demand-side flexibility resources for renewable energy accommodation in electrical power systems. *Front. Energy Res.* 11. <https://doi.org/10.3389/fenrg.2023.1333872>.
- DNV GL, 2022. Definitions of Availability Terms for the Wind Industry. DNV GL. White Pap. 17.
- Doğan, B., Chu, L.K., Ghosh, S., Diep Truong, H.H., Balsalobre-Lorente, D., 2022. How environmental taxes and carbon emissions are related in the G7 economies? *Renew. Energy* 187, 645–656. <https://doi.org/10.1016/j.renene.2022.01.077>.
- Dong, F., Li, Y., Gao, Y., Zhu, J., Qin, C., Zhang, X., 2022. Energy transition and carbon neutrality: Exploring the non-linear impact of renewable energy development on carbon emission efficiency in developed countries. *Resour. Conserv. Recycl.* 177, 106002. <https://doi.org/10.1016/j.resconrec.2021.106002>.
- Donglin, C.U.I., Wei, S.H.A., Shujie, L.I.U., Qiuyang, C., Nina, W., 2023. Case Study of “Wake Effect” of Adjacent Offshore Wind Farms. *South. ENERGY Constr.* 10, 21–28. <https://doi.org/10.16516/j.gedi.issn2095-8676.2023.01.003>.
- Duffie, J.A., Beckman, W.A., Blair, N., 2020. *Solar engineering of thermal processes, photovoltaics and wind*. John Wiley & Sons.
- Dumortier, J., Elobeid, A., 2021. Effects of a carbon tax in the United States on agricultural markets and carbon emissions from land-use change. *Land Use Policy* 103, 105320. <https://doi.org/10.1016/j.landusepol.2021.105320>.
- Engineering Toolbox, 2024. Orifice, Nozzle and Venturi Flow Rate Meters.
- Enphase Energy, 2017. The Enphase AC Battery Data Sheet [WWW Document].
- Erbs, D.G., Klein, S.A., Duffie, J.A., 1982. Estimation of the diffuse radiation fraction for hourly, daily and monthly-average global radiation. *Sol. Energy* 28, 293–302. [https://doi.org/10.1016/0038-092X\(82\)90302-4](https://doi.org/10.1016/0038-092X(82)90302-4).
- Esmailian, B., Sarkis, J., Lewis, K., Behdad, S., 2020. Blockchain for the future of sustainable supply chain management in Industry 4.0. *Resour. Conserv. Recycl.* 163, 105064. <https://doi.org/10.1016/j.resconrec.2020.105064>.
- Fan, C.-K., Potts, J., Castellanos, S., 2025. Offshore wind manufacturing, deployment, and the just transition in Texas. *Renew. Sustain. Energy Rev.* 211, 115292. <https://doi.org/10.1016/j.rser.2024.115292>.
- Ferrari, F., Besio, G., Cassola, F., Mazzino, A., 2020. Optimized wind and wave energy resource assessment and offshore exploitability in the Mediterranean Sea. *Energy* 190, 116447. <https://doi.org/10.1016/j.energy.2019.116447>.
- Flórez-Orrego, D., Freire, R.A., da Silva, J.A.M., Albuquerque Neto, C., de Oliveira Junior, S., 2022. Centralized power generation with carbon capture on decommissioned offshore petroleum platforms. *Energy Convers. Manag.* 252, 115110. <https://doi.org/10.1016/j.enconman.2021.115110>.
- Flórez-Orrego, D., Neto, C.A., da Silva, J.A.M., Freire, R.L.A., de Oliveira, S., 2021. Offshore utility systems for FPSOs: techno-economic, environmental assessment and trade-offs between gas price, carbon taxation and opportunity cost. *ECOS 2021 34th Int. Conf. Efficiency Cost. Optim. Simul. Environ. Impact Energy Syst.* 715–726. <https://doi.org/10.52202/062738-0064>.
- Fofang, T.F., Tanyi, E., 2020. Design and Simulation of Off-Grid Solar/Mini-Hydro Renewable Energy System using Homer Pro Software: Case of Muyuka Rural Community. *Int. J. Eng. Res. Technol.* 9.
- Fofonoff, N.P., Millard, R.C., 1983. Algorithms for computation of fundamental properties of seawater. *UNESCO Tech. Pap. Mar. Sci.* 44, 53.
- Gabbar, H.A., Esteves, O.L.A., 2023. Planning and Evaluation of Nuclear-Renewable Hybrid Energy Penetration for Marine and Waterfront Applications. *Energies* 16. <https://doi.org/10.3390/en16145329>.
- Gatzert, N., Kosub, T., 2016. Risks and risk management of renewable energy projects: The case of onshore and offshore wind parks. *Renew. Sustain. Energy Rev.* 60, 982–998. <https://doi.org/10.1016/j.rser.2016.01.103>.
- Chigo, A., Cottura, L., Caradonna, R., Bracco, G., Mattiazzo, G., 2020. Platform Optimization and Cost Analysis in a Floating Offshore Wind Farm. *J. Mar. Sci. Eng.* 8. <https://doi.org/10.3390/jmse8110835>.
- Chigo, A., Faraggiana, E., Sirigu, M., Mattiazzo, G., Bracco, G., 2022. Design and Analysis of a Floating Photovoltaic System for Offshore Installation: The Case Study of Lampedusa. *Energies* 15. <https://doi.org/10.3390/en15238804>.
- Global Solar Atlas, n.d. Global Solar Atlas - Türkiye [WWW Document]. Energy.info. URL (<https://globalsolaratlas.info/download/turkey>) (accessed 1.7.25).
- Global Wind Atlas, n.d. Global Wind Atlas - Türkiye [WWW Document]. Energy.info. URL (<https://globalwindatlas.info/en/area/Turkey/>) (accessed 1.7.25).
- Golroodbari, S.Z.M., Vaartjes, D.F., Meit, J.B.L., van Hoeken, A.P., Eberverd, M., Jonker, H., van Sark, W.G.J.H.M., 2021. Pooling the cable: A techno-economic feasibility study of integrating offshore floating photovoltaic solar technology within an offshore wind park. *Sol. Energy* 219, 65–74. <https://doi.org/10.1016/j.solener.2020.12.062>.
- Görmüş, T., Aydoğan, B., Ayat, B., 2024. Analysis of hybrid exploitation of wind and wave power in the Mediterranean and the Black Sea. *Energy Convers. Manag.* 299, 117820. <https://doi.org/10.1016/j.enconman.2023.117820>.
- Goswami, A., Sadhu, P., Goswami, U., Sadhu, P.K., 2019. Floating solar power plant for sustainable development: A techno-economic analysis. *Environ. Prog. \ Sustain. Energy* 38, e13268. <https://doi.org/10.1002/ep.13268>.
- Graham, V.A., Hollands, K.G.T., 1990. A method to generate synthetic hourly solar radiation globally. *Sol. Energy* 44, 333–341. [https://doi.org/10.1016/0038-092X\(90\)90137-2](https://doi.org/10.1016/0038-092X(90)90137-2).
- Graham, V.A., Hollands, K.G.T., Unny, T.E., 1988. A time series model for Kt with application to global synthetic weather generation. *Sol. Energy* 40, 83–92. [https://doi.org/10.1016/0038-092X\(88\)90075-8](https://doi.org/10.1016/0038-092X(88)90075-8).
- Gugler, K., Haxhimusa, A., Liebensteiner, M., 2023. Carbon pricing and emissions: Causal effects of Britain's carbon tax. *Energy Econ.* 121, 106655. <https://doi.org/10.1016/j.eneco.2023.106655>.

- GUINARD Energies, 2017. POSEIDE 66 - RIVER AND MARINE CURRENT TURBINE [WWW Document].
- Hariga, M., As'ad, R., Shamayleh, A., 2017. Integrated economic and environmental models for a multi stage cold supply chain under carbon tax regulation. *J. Clean. Prod.* 166, 1357–1371. <https://doi.org/10.1016/j.jclepro.2017.08.105>.
- He, Q., Chen, H., Lin, Z., Dai, X., Huang, Y., Cai, W., 2022. A cost-based life-cycle pricing model for offshore wind power plants within China's carbon trading scheme. *Energy Rep.* 8, 147–155. <https://doi.org/10.1016/j.egy.2022.08.101>.
- HOMER Energy, n.d. HOMER Pro Documentation [WWW Document]. HOMER Pro 3.15. URL (https://homerenergy.com/products/pro/docs/3.15/how_homer_calculates_the_pv_array_power_output.html) (accessed 1.7.25).
- HOMER Pro Manuel Help [WWW Document], 2025.
- Huang, J., Iglesias, G., 2024. Hybrid offshore wind-solar energy farms: A novel approach through retrofitting. *Energy Convers. Manag.* 319, 118903. <https://doi.org/10.1016/j.enconman.2024.118903>.
- International Energy Agency, 2023. Carbon Pricing and Taxation: 2023 Update.
- İpekli, Z., Keskin, S., Genç, M.S., Genç, G., 2024. Offshore and onshore renewable energy system modelling to meet the energy demand of megacity Istanbul. *Process Saf. Environ. Prot.* 190, 34–45. <https://doi.org/10.1016/j.psep.2024.08.011>.
- Iqbar, I.M., Muhammad, M., Gilani, S.I.U.-H., Adam, F., 2022. Feasibility Study of Harnessing Low Wind Speed Turbine as Hybrid Power Source for Offshore Platforms. *J. Mar. Sci. Eng.* 10. <https://doi.org/10.3390/jmse10070963>.
- IRENA and ILO, 2022. Renewable Energy and Jobs Annual Review 2022, International Renewable Energy Agency (IRENA) and International Labour Organization (ILO).
- Izquierdo-Pérez, J., Brentan, B.M., Izquierdo, J., Clausen, N.-E., Pegalajar-Jurado, A., Ebsen, N., 2020. Layout Optimization Process to Minimize the Cost of Energy of an Offshore Floating Hybrid Wind-Wave Farm. *Processes* 8. <https://doi.org/10.3390/pr8020139>.
- Jamroen, C., 2022. Optimal techno-economic sizing of a standalone floating photovoltaic/battery energy storage system to power an aquaculture aeration and monitoring system. *Sustain. Energy Technol. Assess.* 50, 101862. <https://doi.org/10.1016/j.seta.2021.101862>.
- Jiang, H., Yao, L., Zhou, C., 2023. Assessment of offshore wind-solar energy potentials and spatial layout optimization in mainland China. *Ocean Eng.* 287, 115914. <https://doi.org/10.1016/j.oceaneng.2023.115914>.
- Kafeel, K., Zhou, J., Phetkhammai, M., Heyan, L., Khan, S., 2024. Green innovation and environmental quality in OECD countries: the mediating role of renewable energy and carbon taxes. *Environ. Sci. Pollut. Res.* 31, 2214–2227. <https://doi.org/10.1007/s11356-023-31111-5>.
- Kangaji, L.M., Raji, A., Orumwense, E., 2024. Optimizing Sustainability Offshore Hybrid Tidal-Wind Energy Storage Systems for an Off-Grid Coastal City in South Africa. *Sustainability* 16. <https://doi.org/10.3390/su16219139>.
- Kazemi-Robati, E., Silva, B., Bessa, R.J., 2024. Stochastic optimization framework for hybridization of existing offshore wind farms with wave energy and floating photovoltaic systems. *J. Clean. Prod.* 454, 142215. <https://doi.org/10.1016/j.jclepro.2024.142215>.
- Khan, K., 2025. How do supply chain and geopolitical risks threaten energy security? A time and frequency analysis. *Energy* 316, 134501. <https://doi.org/10.1016/j.energy.2025.134501>.
- Khare, V., Khare, C.J., Bhuiyan, M.A., 2023. Design, optimization, and data analysis of solar-tidal hybrid renewable energy system for Hurawalhi, Maldives. *Clean. Energy Syst.* 6, 100088. <https://doi.org/10.1016/j.cles.2023.100088>.
- Khastar, M., Aslani, A., Nejati, M., 2020. How does carbon tax affect social welfare and emission reduction in Finland? *Energy Rep.* 6, 736–744. <https://doi.org/10.1016/j.egy.2020.03.001>.
- Khurshid, H., Mohammed, B.S., Al-Yacoubi, A.M., Liew, M.S., Zawawi, N.A.W.A., 2024. Analysis of hybrid offshore renewable energy sources for power generation: A literature review of hybrid solar, wind, and waves energy systems. *Dev. Built Environ.* 19, 100497. <https://doi.org/10.1016/j.dibe.2024.100497>.
- Kim, J.-H., Nam, I., Kang, S., Jung, S., 2022. Development of an Optimized Curtailment Scheme through Real-Time Simulation. *Energies* 15. <https://doi.org/10.3390/en15031074>.
- Kowsar, A., Hassan, M., Rana, M.T., Haque, N., Faruque, M.H., Ahsan, S., Alam, F., 2023. Optimization and techno-economic assessment of 50 MW floating solar power plant on Hakaluki marsh land in Bangladesh. *Renew. Energy* 216, 119077. <https://doi.org/10.1016/j.renene.2023.119077>.
- Lee, J.C.Y., Fields, M.J., 2021. An overview of wind-energy-production prediction bias, losses, and uncertainties. *Wind Energy Sci.* 6, 311–365. <https://doi.org/10.5194/wes-6-311-2021>.
- Leimeister, M., Kolios, A., 2018. A review of reliability-based methods for risk analysis and their application in the offshore wind industry. *Renew. Sustain. Energy Rev.* 91, 1065–1076. <https://doi.org/10.1016/j.rser.2018.04.004>.
- Lerch, M., De-Prada-Gil, M., Molins, C., 2018. A simplified model for the dynamic analysis and power generation of a floating offshore wind turbine. *E3S Web Conf.* 61, 1–8. <https://doi.org/10.1051/e3sconf/20186100001>.
- Li, M., Cao, S., Zhu, X., Xu, Y., 2022a. Techno-economic analysis of the transition towards the large-scale hybrid wind-tidal supported coastal zero-energy communities. *Appl. Energy* 316, 119118. <https://doi.org/10.1016/j.apenergy.2022.119118>.
- Li, M., Luo, H., Zhou, S., Senthil Kumar, G.M., Guo, X., Law, T.C., Cao, S., 2022b. State-of-the-art review of the flexibility and feasibility of emerging offshore and coastal ocean energy technologies in East and Southeast Asia. *Renew. Sustain. Energy Rev.* 162, 112404. <https://doi.org/10.1016/j.rser.2022.112404>.
- Lilas, T., Dagkinis, I., Stefanakou, A.-A., Antoniou, E., Nikitakos, N., Maglara, A., Vatisstas, A., 2022. Energy utilisation strategy in an offshore floating wind system with variable production of fresh water and hybrid energy storage. *Int. J. Sustain. Energy* 41, 1572–1590. <https://doi.org/10.1080/14786451.2022.2067160>.
- Liu, J., Bai, J., Deng, Y., Chen, X., Liu, X., 2021. Impact of energy structure on carbon emission and economy of China in the scenario of carbon taxation. *Sci. Total Environ.* 762, 143093. <https://doi.org/10.1016/j.scitotenv.2020.143093>.
- Logan, E., 1981. Wind turbines. <https://doi.org/10.4324/9780203103289-9>.
- López, M., Rodríguez, N., Iglesias, G., 2020. Combined Floating Offshore Wind and Solar PV. *J. Mar. Sci. Eng.* 8. <https://doi.org/10.3390/jmse8080576>.
- Luo, W., Isukapalli, S.N., Vinayagam, L., Ting, S.A., Pravettoni, M., Reindl, T., Kumar, A., 2021. Performance loss rates of floating photovoltaic installations in the tropics. *Sol. Energy* 219, 58–64. <https://doi.org/10.1016/j.solener.2020.12.019>.
- Luo, R., Zhou, L., Song, Y., Fan, T., 2022. Evaluating the impact of carbon tax policy on manufacturing and remanufacturing decisions in a closed-loop supply chain. *Int. J. Prod. Econ.* 245, 108408. <https://doi.org/10.1016/j.ijpe.2022.108408>.
- Lüth, A., Keles, D., 2024. Risks, strategies, and benefits of offshore energy hubs: A literature-based survey. *Renew. Sustain. Energy Rev.* 203, 114761. <https://doi.org/10.1016/j.rser.2024.114761>.
- Majdi Nasab, N., Kilby, J., Bakhtiarfard, L., 2021. Case Study of a Hybrid Wind and Tidal Turbines System with a Microgrid for Power Supply to a Remote Off-Grid Community in New Zealand. *Energies* 14. <https://doi.org/10.3390/en14123636>.
- Mäkitie, T., Andersen, A.D., Hanson, J., Normann, H.E., Thune, T.M., 2018. Established sectors expediting clean technology industries? The Norwegian oil and gas sector's influence on offshore wind power. *J. Clean. Prod.* 177, 813–823. <https://doi.org/10.1016/j.jclepro.2017.12.209>.
- Malik, T.H., Bak, C., 2025. Challenges in detecting wind turbine power loss: the effects of blade erosion, turbulence, and time averaging. *Wind Energy Sci.* 10, 227–243. <https://doi.org/10.5194/wes-10-227-2025>.
- Manupati, V.K., Schoenherr, T., Ramkumar, M., Wagner, S.M., Pabba, S.K., Singh, R.I.R., 2020. A blockchain-based approach for a multi-echelon sustainable supply chain. *Int. J. Prod. Res.* 58, 2222–2241. <https://doi.org/10.1080/00207543.2019.1683248>.
- Manwell, J.F., McGowan, J.G., 1993. Lead acid battery storage model for hybrid energy systems. *Sol. Energy* 50, 399–405. [https://doi.org/10.1016/0038-092X\(93\)90060-2](https://doi.org/10.1016/0038-092X(93)90060-2).
- Martinez, A., Iglesias, G., 2021. Multi-parameter analysis and mapping of the levelised cost of energy from floating offshore wind in the Mediterranean Sea. *Energy Convers. Manag.* 243, 114416. <https://doi.org/10.1016/j.enconman.2021.114416>.
- Martinez, A., Iglesias, G., 2022. Site selection of floating offshore wind through the levelised cost of energy: A case study in Ireland. *Energy Convers. Manag.* 266, 115802. <https://doi.org/10.1016/j.enconman.2022.115802>.
- Martinez, A., Iglesias, G., 2024a. Levelised cost of energy to evaluate the economic viability of floating offshore wind in the European Atlantic and Mediterranean. *ePrime Adv. Electr. Eng. Electron. Energy* 8, 100562. <https://doi.org/10.1016/j.priime.2024.100562>.
- Martinez, A., Iglesias, G., 2024b. Mapping of the levelised cost of energy from floating solar PV in coastal waters of the European Atlantic, North Sea and Baltic Sea. *Sol. Energy* 279, 112809. <https://doi.org/10.1016/j.solener.2024.112809>.
- Meng, X., Yu, Y., 2023. Can renewable energy portfolio standards and carbon tax policies promote carbon emission reduction in China's power industry? *Energy Policy* 174, 113461. <https://doi.org/10.1016/j.enpol.2023.113461>.
- Minister of Energy and Mineral Resources of the Republic of Indonesia, 2015. Reencana Usaha Penyediaan Tenaga Listrik PT PLN (Persero) 2015–2024. Persero and Tahun.
- Mirzaei, P.A., Olsthoorn, D., Torjan, M., Haghighat, F., 2015. Urban neighborhood characteristics influence on a building indoor environment. *Sustain. Cities Soc.* 19, 403–413. <https://doi.org/10.1016/j.scs.2015.07.008>.
- Moosavian, S.F., Zahedi, R., Hajinezhad, A., 2022. Economic, Environmental and Social Impact of Carbon Tax for Iran: A Computable General Equilibrium Analysis. *Energy Sci. \ Eng.* 10, 13–29. <https://doi.org/10.1002/ese3.1005>.
- NASA, n.d. Prediction of Worldwide Energy Resource (POWER) database [WWW Document]. NASA Surf. Methodol. Lab. URL (<https://power.larc.nasa.gov/>) (accessed 9.25.24).
- Neill, S.P., Angeloudis, A., Robins, P.E., Walkington, I., Ward, S.L., Masters, I., Lewis, M. J., Piano, M., Avdis, A., Piggott, M.D., Aggidis, G., Evans, P., Adcock, T.A.A., Židonis, A., Ahmadian, R., Falconer, R., 2018. Tidal range energy resource and optimization – Past perspectives and future challenges. *Renew. Energy* 127, 763–778. <https://doi.org/10.1016/j.renene.2018.05.007>.
- Neshat, M., Sergiienko, N.Y., da Silva, L.S.P., Amini, E., Nasiri, M., Mirjalili, S., 2024. Chapter 22 - Adaptive bi-level whale optimization algorithm for maximizing the power output of hybrid wave-wind energy site. In: Mirjalili, S. (Ed.), *Handbook of Whale Optimization Algorithm*. Academic Press, pp. 291–308. <https://doi.org/10.1016/B978-0-32-395365-8.00028-2>.
- NOAA, 2025. Tides and Currents Data for Indonesian Coastal Rivers.
- Nong, D., Simshauser, P., Nguyen, D.B., 2021. Greenhouse gas emissions vs CO2 emissions: Comparative analysis of a global carbon tax. *Appl. Energy* 298, 117223. <https://doi.org/10.1016/j.apenergy.2021.117223>.
- Nyiwul, L., Koirala, N.P., 2024. Renewable energy policy performance and technological innovation in Africa: A Bayesian estimation. *Energy Policy* 193, 114279. <https://doi.org/10.1016/j.enpol.2024.114279>.
- Onwe, J.C., Bandyopadhyay, A., Hamid, I., Rej, S., Hossain, M.E., 2023. Environment sustainability through energy transition and globalization in G7 countries: What role does environmental tax play? *Renew. Energy* 218, 119302. <https://doi.org/10.1016/j.renene.2023.119302>.
- Organisation for Economic Co-operation and Development (OECD), 2023. Effective Carbon Rates 2023: Pricing Carbon Emissions Through Taxes and Emissions Trading. Paris. <https://doi.org/10.1787/58a09c74-en>.

- Ozturk, Z., Terkes, M., Demirci, A., 2024. Optimal planning of hybrid power systems under economic variables and different climatic regions: A case study of Türkiye. *Renew. Energy* 232, 121029. <https://doi.org/10.1016/j.renene.2024.121029>.
- Petracca, E., Faraggiana, E., Ghigo, A., Sirigu, M., Bracco, G., Mattiazzi, G., 2022. Design and Techno-Economic Analysis of a Novel Hybrid Offshore Wind and Wave Energy System. *Energies* 15. <https://doi.org/10.3390/en15082739>.
- Pryor, S.C., Barthelmie, R.J., 2024. Wind shadows impact planning of large offshore wind farms. *Appl. Energy* 359, 122755. <https://doi.org/10.1016/j.apenergy.2024.122755>.
- PT PLN (Persero), n.d. Electricity Tariff in Indonesia [WWW Document]. URL (http://web.pln.co.id/static/uploads/2021/06/tf_april_juni_2021.pdf) (accessed 10.22.24).
- Rahaman, M.A., Chambers, T.L., Fekih, A., Wiecheteck, G., Carranza, G., Possetti, G.R.C., 2023. Floating photovoltaic module temperature estimation: Modeling and comparison. *Renew. Energy* 208, 162–180. <https://doi.org/10.1016/j.renene.2023.03.076>.
- Ramesh, M., Saini, R.P., 2020. Dispatch strategies based performance analysis of a hybrid renewable energy system for a remote rural area in India. *J. Clean. Prod.* 259, 120697. <https://doi.org/10.1016/j.jclepro.2020.120697>.
- Ramos-Marín, S., Caio, A., Guedes Soares, C., 2024. Optimization of a hybrid electricity system in the Canary Islands including marine renewable energies. *Int. Hybrid. Power Plants Syst. Workshop (HYB 2024)* 337–353. <https://doi.org/10.1049/icp.2024.1860>.
- Rasool, S., Muttaqi, K.M., Sutanto, D., 2022. A Novel Configuration of a Hybrid Offshore Wind-Wave Energy Conversion System and Its Controls for a Remote Area Power Supply. *IEEE Trans. Ind. Appl.* 58, 7805–7817. <https://doi.org/10.1109/TIA.2022.3197099>.
- Rasool, S., Muttaqi, K.M., Sutanto, D., 2023. An Investigation on the Integration of a Hybrid Offshore Wind-Wave Energy Conversion System With the Distribution Network. *IEEE Trans. Ind. Appl.* 59, 4562–4571. <https://doi.org/10.1109/TIA.2023.3268225>.
- Rönkkö, J., Khosravi, A., Syri, S., 2023. Techno-Economic Assessment of a Hybrid Offshore Wind-Wave Farm: Case Study in Norway. *Energies* 16. <https://doi.org/10.3390/en16114316>.
- Rubio-Domingo, G., Linares, P., 2021. The future investment costs of offshore wind: An estimation based on auction results. *Renew. Sustain. Energy Rev.* 148, 111324. <https://doi.org/10.1016/j.rser.2021.111324>.
- Sabine, G., Avotra, N., Olivia, R., Sandrine, S., 2020. A macroeconomic evaluation of a carbon tax in overseas territories: A CGE model for Reunion Island. *Energy Policy* 147, 111738. <https://doi.org/10.1016/j.enpol.2020.111738>.
- Satymov, R., Bogdanov, D., Dadashi, M., Lavidas, G., Breyer, C., 2024. Techno-economic assessment of global and regional wave energy resource potentials and profiles in hourly resolution. *Appl. Energy* 364, 123119. <https://doi.org/10.1016/j.apenergy.2024.123119>.
- Schetingner, A.M., Bozelli, H.B., Amaral, J.M.T. do, Souza, C.C.M. de, Pereira, A.O., Alves, A.G.P., Emmerik, van, E.L., Silva, G. de J., Cambruzzi, P.H.B., Dias, R.F. da S., 2025. Floating Offshore Wind and Carbon Credits in Brazil: A Case Study on Floating Production, Storage and Offloading Unit Decarbonization. *Resources* 14. <https://doi.org/10.3390/resources14060085>.
- Sergio Campobasso, M., Castorini, A., Ortolani, A., Minisci, E., 2023. Probabilistic analysis of wind turbine performance degradation due to blade erosion accounting for uncertainty of damage geometry. *Renew. Sustain. Energy Rev.* 178, 113254. <https://doi.org/10.1016/j.rser.2023.113254>.
- Smith, I.D., 2020. How the process of transitions shapes the politics of decarbonization: Tracing policy feedback effects across phases of the energy transition. *Energy Res. Soc. Sci.* 70, 101753. <https://doi.org/10.1016/j.erss.2020.101753>.
- Smith, D.C., 2023. Geopolitical realities of the energy transition supply chain: energy security risks and opportunities. *J. Energy \ Nat. Resour. Law* 41, 233–239. <https://doi.org/10.1080/02646811.2023.2230732>.
- Smith, K., Earleywine, M., Wood, E., Neubauer, J., Pesaran, A., 2012. Comparison of plug-in hybrid electric vehicle battery life across geographies and drive cycles. *SAE Tech. Pap.* <https://doi.org/10.4271/2012-01-0666>.
- Terkes, M., Arian, O., Gokalp, E., 2024a. The effect of electric vehicle charging demand variability on optimal hybrid power systems with second-life lithium-ion or fresh Na-S batteries considering power quality. *Energy* 288, 129760. <https://doi.org/10.1016/j.energy.2023.129760>.
- Terkes, M., Demirci, A., Gokalp, E., 2023. An evaluation of optimal sized second-life electric vehicle batteries improving technical, economic, and environmental effects of hybrid power systems. *Energy Convers. Manag.* 291, 117272. <https://doi.org/10.1016/j.enconman.2023.117272>.
- Terkes, M., Demirci, A., Gokalp, E., Cali, U., 2024b. Multi-stage and multi-objective feed-in damping-based battery aging-aware energy management strategy for renewable energy integration. *IEEE Access* 11. <https://doi.org/10.1109/ACCESS.2024.3468716>.
- Terkes, M., Demirci, A., Ozturk, Z., Cali, U., 2024c. Strategic Integration of Second-Life Batteries: Incentive Mechanisms for Boosting Community Energy Self-Consumption. *IEEE Access* 12, 125768–125785. <https://doi.org/10.1109/ACCESS.2024.3429578>.
- Toms, A.M., Li, X., Rajashekara, K., 2023. Optimal Sizing of On-Site Renewable Resources for Offshore Microgrids, in: 2023. North Am. Power Symp (NAPS) 1–6. <https://doi.org/10.1109/NAPS58826.2023.10318718>.
- Toumi, S., Amirat, Y., Elbouchikhi, E., Zhou, Z., Benbouzid, M., 2023. Techno-Economic Optimal Sizing Design for a Tidal Stream Turbine–Battery System. *J. Mar. Sci. Eng.* 11. <https://doi.org/10.3390/jmse11030679>.
- Varotto, S., Trovato, V., Kazemi-Robati, E., Silva, B., 2024. Optimal Sizing and Energy Management of Battery Energy Storage Systems for Hybrid Offshore Farms. *IEEE 22nd Mediterr. Electrotech. Conf. (MELECON)* 390–395. <https://doi.org/10.1109/MELECON56669.2024.10608500>.
- Vázquez, R., Cabos, W., Nieto-Borge, J.C., Gutiérrez, C., 2024. Complementarity of offshore energy resources on the Spanish coasts: Wind, wave, and photovoltaic energy. *Renew. Energy* 224, 120213. <https://doi.org/10.1016/j.renene.2024.120213>.
- Wang, X., Khurshid, A., Qayyum, S., Calin, A.C., 2022. The role of green innovations, environmental policies and carbon taxes in achieving the sustainable development goals of carbon neutrality. *Environ. Sci. Pollut. Res.* 29, 8393–8407. <https://doi.org/10.1007/s11356-021-16208-z>.
- Wang, C., Wang, W., Huang, R., 2017. Supply chain enterprise operations and government carbon tax decisions considering carbon emissions. *J. Clean. Prod.* 152, 271–280. <https://doi.org/10.1016/j.jclepro.2017.03.051>.
- Wang, J., Zhou, S., Li, M., Ren, G., Ren, X., Xiong, X., Zhang, Y., 2025. Multi-echelon inventory optimization of waste electrical and electronic equipment closed-loop supply chain based on reinforcement learning under carbon tax policy. *Eng. Appl. Artif. Intell.* 154, 110987. <https://doi.org/10.1016/j.engappai.2025.110987>.
- Wen, Y., Lin, P., 2024. Offshore solar photovoltaic potential in the seas around China. *Appl. Energy* 376, 124279. <https://doi.org/10.1016/j.apenergy.2024.124279>.
- Wikipedia contributors, 2024. Seagreen Offshore Wind Farm.
- Wilkie, D., Galasso, C., 2020. A probabilistic framework for offshore wind turbine loss assessment. *Renew. Energy* 147, 1772–1783. <https://doi.org/10.1016/j.renene.2019.09.043>.
- World Bank, 2024. State and Trends of Carbon Pricing 2024. World Bank Publ.
- Xu, H., Pan, X., Li, J., Feng, S., Guo, S., 2023. Comparing the impacts of carbon tax and carbon emission trading, which regulation is more effective? *J. Environ. Manag.* 330, 117156. <https://doi.org/10.1016/j.jenvman.2022.117156>.
- Yang, S., Yuan, J., Nian, V., Li, L., Li, H., 2022. Economics of marinated offshore charging stations for electrifying the maritime sector. *Appl. Energy* 322, 119389. <https://doi.org/10.1016/j.apenergy.2022.119389>.
- Yüksel, O., Konur, O., Pamik, M., Bayraktar, M., 2024. The economic and environmental assessment of alternative marine fuels and nuclear energy utilization on a floating power plant. *Environ. Sci. Pollut. Res.* 31, 49780–49799. <https://doi.org/10.1007/s11356-024-34532-y>.
- Zaman, M.A., Ongsakul, W., 2022. Hybrid Microgrid Optimization for Smart City Planning on Saint Martin's Island in Bangladesh. *Int. Conf. Util. Exhib. Energy Environ. Clim. Change (ICUE)* 1–16. <https://doi.org/10.1109/ICUE55325.2022.10113498>.
- Zhang, R., Shen, G.Q.P., Ni, M., Wong, J.K.W., 2019. An overview on the status quo of onshore and offshore wind power development and wind power enterprise localization in China. *Int. J. Green. Energy* 16, 1646–1664. <https://doi.org/10.1080/15435075.2019.1681429>.
- Zhang, H., Tomasgard, A., Knudsen, B.R., Svendsen, H.G., Bakker, S.J., Grossmann, I.E., 2022. Modelling and analysis of offshore energy hubs. *Energy* 261, 125219. <https://doi.org/10.1016/j.energy.2022.125219>.
- Zhang, C., Xu, Y., Zheng, Y., 2024. Blockchain Traceability Adoption in Low-Carbon Supply Chains: An Evolutionary Game Analysis. *Sustainability* 16. <https://doi.org/10.3390/su16051817>.
- Zhao, Z.-Y., Hao, Y.-X., Chang, R.-D., Wang, Q.-C., 2023. Assessing the vulnerability of energy supply chains: Influencing factors and countermeasures. *Sustain. Energy Technol. Assess.* 56, 103018. <https://doi.org/10.1016/j.seta.2023.103018>.
- Zhou, Y., 2023. Worldwide carbon neutrality transition? Energy efficiency, renewable, carbon trading and advanced energy policies. *Energy Rev.* 2, 100026. <https://doi.org/10.1016/j.enrev.2023.100026>.
- Zhou, S., Cao, S., Wang, S., 2022. Realisation of a coastal zero-emission office building with the support of hybrid ocean thermal, floating photovoltaics, and tidal stream generators. *Energy Convers. Manag.* 253, 115135. <https://doi.org/10.1016/j.enconman.2021.115135>.
- Zhu, N., Bu, Y., Jin, M., Mbrog, N., 2020. Green financial behavior and green development strategy of Chinese power companies in the context of carbon tax. *J. Clean. Prod.* 245, 118908. <https://doi.org/10.1016/j.jclepro.2019.118908>.